FIRE PERFORMANCE OF HYBRID FIBER REINFORCED SELF CONSOLIDATING CONCRETE (HFRSCC) WITH GLASS POZZOLAN

By

RISHABH KUMAR

Presented to the Faculty of the Graduate School of
The University of Texas at Arlington in Partial Fulfillment
of the Requirements
for the Degree of

MASTER OF SCIENCE IN CIVIL ENGINEERING

THE UNIVERSITY OF TEXAS AT ARLINGTON

December 2021

Copyright © by Rishabh Kumar 2021

All Rights Reserved

Acknowledgments

Firstly, I would like to thank my advising professor Dr. Nur Yazdani, for this great opportunity to join his research team, for his unconditional support and guidance throughout this research. It has been a privilege working under him and with his spectacular research group, I am truly grateful for this experience. I would also like to thank my committee members, Dr. Himan Hojat Jalali, and Dr. Kyeong Ruk Ryu for reviewing my work and providing the necessary guidance.

Sincere thanks to Dr. Eyosias Beneberu Solomon for being an inspiring personality, helping me with the research, consistently reviewing my work, and providing necessary criticism and skepticism.

I want to thank my family members, my parents, Vijay Kumar Shah and Usha Shah, my brother, Vishal Kumar Shah, for always believing in me, motivating me to strive and achieve better in life.

I also thank James Robb from Euclid Chemicals for supporting my research and providing me the necessary raw materials required to carry-out the research work.

This have been a tremendous experience, with a lot of hard work and patience. Regardless of the difficulties, there is a high sense of satisfaction and achievement in the end. I thank everyone who has been a part of this project and has made it possible.

October 25, 2021

Abstract

FIRE PERFORMANCE OF HYBRID FIBER REINFORCED SELF CONCOLIDATING CONCRETE (HFRSCC) WITH GLASS POZZOLAN

Rishabh Kumar. M.S.

The University of Texas at Arlington, 2020

Supervising professor: Nur Yazdani, PhD

This research focusses on the effects of hybridizing self-consolidating concrete (SCC) using steel (SF) and polypropylene (PP) fibers to study their benefits post fire exposure. In an attempt to reduce cement's environmental impacts and to make concrete more sustainable, this research also studies substitution of cement using glass pozzolan. Limited research has been done in this regard previously, hence this research makes an effort to bridge the enormous knowledge gap. No research has reported tensile, compressive, and flexural strength of SCC with hybrid fibers and glass pozzolan, making this research unique. Based on previous research, replacement rate of cement by glass pozzolan used is 20%. The dosage rates of steel and polypropylene fibers are 3.5 lb./yd^3 and 1.5 lb./yd^3. Four different SCC mixes are designed with different combinations of glass pozzolan and hybrid fibers. A total of 12 beams (three for each SCC mix) and 24 cylinders (six for each SCC mix) are tested as per ASTM standards. Out of the 12 beams, four were tested at room temperature and the remaining eight were tested after 30 minutes of fire exposure as per the ASTM E119 (2019) standards. Similarly, eight cylinders were tested at room temperature and the rest after fire exposure. No benefits of adding hybrid fibers were observed for compressive strength at both room and elevated temperatures. Split tensile strength of cylinders after fire exposure was found to be higher for the specimens containing hybrid fibers. At room temperature, flexural strength of control SCC was found to be the highest while other mixes reported lesser strength. Post fire exposure, flexural strength

of mixes containing hybrid fibers reported much better strength than control specimens. Also, brittle failure observed at room temperature was found to be ductile at elevated temperature for mixes containing hybrid fibers and/or glass pozzolan. Fibers did not aid these strength parameters at room temperature but had better results post fire exposure.

Table of Contents

List of Figures

List of Tables

Chapter 1

Introduction

1.1 Background

Strengthening of concrete remains a pressing challenge for the construction industry to meet on-field demands. Since structures are subject to varying field conditions, environmental phenomenon, and hazardous situations, there is a constant demand for improvement in concrete. Therefore, the industry always strives to increase the performance of concrete, which has led to different versions of concrete, including Reinforced Concrete (RC), Prestressed Concrete (PC), Air – Entrained Concrete, Rapid set Concrete, and Fiber Reinforced Concrete (FRC).

FRC is an older technique with roots in the ancient times, and in the 1900s, asbestos fibers were used in concrete to reduce cracks. In the 1960s, various other fibers like steel, glass, and synthetic fibers, such as polypropylene were discovered. The main justification for the use of fibers to reinforce concrete is to control cracks from plastic shrinkage and drying shrinkage, though fibers also provide other benefits. Some of the different types of fiber reinforced concretes include the following:

1.) Steel Fiber Reinforced Concrete (SFRC)
2.) Glass Fiber Reinforced Concrete (GFRC)
3.) Polypropylene Fiber Reinforced Concrete (PFRC)
4.) Carbon Fiber Reinforced Concrete (CFRC)

Steel fiber (SF) reinforced concrete is produced by blending steel fibers in the concrete mix. Steel fibers additionally help to enhance the tensile, compressive, and flexural strength of concrete, thereby preventing the microcracks due to drying shrinkage and thermal contractions

to form into larger cracks, making concrete more ductile. Moreover, steel fibers make concrete more stable against thermal variations and give better residual properties after fire exposure.

Glass fiber reinforced concrete, on the other hand, is a blend of glass fibers in concrete mix. Since glass is abundantly available today, recycling the glass and using it to reinforce concrete would be an economical and environment-friendly solution. Glass fiber also proves to be beneficial in terms of its lightweight construction, increased strength, and fire resistance (Crafting with Concrete, 2021).

The next type of fiber reinforced concrete uses Polypropylene (PP) fibers; these are micro synthetic fibers effectively known for their fire-resistant properties. Additional benefits include reduction to water penetration, reduction in plastic shrinkage cracking and propagation of cracks. Other synthetic fiber types are polyethylene, polyester, poly vinyl alcohol, and nylon fibers.

The carbon fibers used in Carbon Fiber Reinforced Concrete (CFRC) are the most recent addition to the fiber family. Carbon fibers are known to have a high modulus of elasticity and flexural strength. Their strength characteristics are superior to those of steel; however, they are highly prone to damage. Generally, carbon fibers are coated with resin before being used as reinforcement (Mishra, 2021). Figure 1 shows some of the fibers.

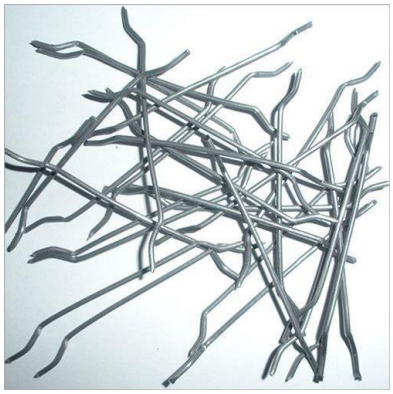

a.

b.

c.

d.

Figure 1: Fibers used in concrete reinforcement: a) Steel fibers; b) Glass fibers; c) Polypropylene fibers; d) Carbon fibers

Many of the fibers used to reinforce concrete, unfortunately have limited benefits to the concrete mix. Steel fiber only enhanced mechanical properties of the concrete but did not provide sufficient resistance to crack formation and propagation. Glass fibers are known to enhance durability and produces lightweight concrete mix, but it is known to lose its strength over a long period of time and can be costlier than concrete (Crafting with Concrete, 2021). On the other hand, polypropylene fibers provide appropriate resistance to crack formation and propagation but have no positive effects on the strength parameters. If used in excess, polypropylene fibers have shown a reduction in strength parameters.

Overall, the limited application of fibers when used individually has given rise to the concept of *hybridization*. *Hybridization* is the process in which concrete is reinforced with two different types of fibers simultaneously, incorporating the individual benefits of the fibers to the mix as a synergy. The commonly used combinations are steel and polypropylene fibers, steel and polyethylene fibers, glass and carbon fibers, glass and basalt fibers, and glass and nylon fibers. The present study focuses on the synergy of steel and polypropylene fibers in the concrete mix.

Self-Consolidating Concrete (SCC) is known to flow under its own weight and does not require any mechanical vibration; therefore, it has gained popularity in the construction industry over the years. SCC is preferred in the design of complex structures as it can move easily and fill congested regions and complex formworks in addition to offering more freedom in construction. Since SCC can flow under its own weight, it can be easily casted assisting in faster construction when compared to normal vibrated concrete. SCC additionally has better structural integrity, pumpability, consolidation, and this type of concrete is a cost-effective option. Accordingly, the present study aims to explore the benefits that SCC can offer post fire exposure when concrete is reinforced with hybrid fibers.

The United States (U.S.) is believed to be the fourth largest cement producing country in the world, with 900 million metric tons produced in 2020 (Statista, 2021). Manufacturing of Portland cement, the most common type of cement, results in emission of anthropogenic carbon dioxide. Additionally, 5% of total CO_2 emissions in the world are caused by cement manufacturing, and 2% of the total CO_2 emissions in the US are from the cement industry (Ehrlich, 2010).

Owing to the impact of excessive CO_2 emissions on global warming, there is a significant need to reduce cement consumption in the construction industry. Attempts have been previously made to reduce cement consumption by replacing cement with materials such as supplementary cementitious materials (SCMs), mineral admixtures, and pozzolans. Some of the more effective cement replacements include Ground Granulated Blast Furnace Slag (GGBS), silica fumes, limestone, fly ash, and natural pozzolans.

Fly ash is a highly preferred cement replacement material as it provides benefits such as greater workability and a general reduction of the water-cement ratio, heat of hydration, cracks, permeability, and bleeding. Fly ash is a less environmentally harmful option. Fly ash, a

byproduct of burning pulverized coal, is a pozzolan containing aluminous and siliceous material that forms cement when mixed with water. The quality of fly ash used is of utmost significance, and the use of poor-quality fly ash has negative effects on concrete such as slower strength gains, increased need for air-entraining admixtures (Rodriguez, 2021).

Furthermore, the construction industry has recently been facing a shortage in the supply of fly ash. While McCormick and Robl (2021) stated that there is enough fly ash available in the US, most of it is either unusable or not present at the right location. Fly ash is also a heavy material, making it costly to transport. Consequently, there is a regional shortage in the fly ash supply. Hence there is a need to substitute fly ash with another pozzolan, such as Glass Pozzolan (GP). The present study aims to explore the substitution of fly ash as a cement replacement using glass pozzolans and the incorporation of glass pozzolans in the concrete mix design.

1.2 Problem Statement

Currently, there is limited research on hybrid fiber reinforced concrete and, specifically, its exposure to fire. Only a small number of studies (Ding et. al 2012; Mahapatra et. al 2019; Varona et. al, 2018; Wu et al, 2020)) focus on the hybrid effect of steel and polypropylene fibers on the concrete mix. Although hybridization is an effective approach to enhance concrete's performance, hybridization's ability to mitigate fire hazards is uncertain. Therefore, more research is necessary to better understand the behavior of hybridized concrete mix.

Another concern is the increased global consumption of cement and the resulting ecological effects. To make concrete more eco-friendly, effective cement replacement measures are crucial. The replacement of cement with glass pozzolan in a self-consolidating concrete mix has not been adequately explored in the existing body of research. This study aims to bridge the research gap and explore effective approaches to replace cement with glass

pozzolan for a SCC design mix.

1.3 Objectives

- Synthesize existing literature to investigate various types of concrete, fiber dosage rates, and cement replacement rates.
- Design four concrete mixes with the appropriate amount of fiber dosage and cement replacement.
- Conduct trials to obtain the appropriate mix design, complying with the standard design specifications.
- Prepare and cast samples with the hybrid fiber reinforced concrete mix.
- Expose the specimens to fire and perform pre-determined tests on samples.
- Quantify and compare the results of the hybrid fiber mix and the control mix, to subsequently compare the results with previous similar studies.
- Draw conclusions and quantify the effectiveness of hybrid fiber-reinforced concrete against fire.
- Provide recommendations for future research needs.

Chapter 2

Literature Review

2.1 Vibrated Concrete (VC) vs Self Consolidating Concrete at Elevated Temperature

In general, when concrete is exposed to elevated temperatures it undergoes mechanical and chemical changes. Mechanical changes include spalling and external cracking whereas chemical changes typically involve discoloration, aggregate changes, or carbonation (Whitley, 2019). External cracking is caused by thermal expansion and dehydration of concrete. Discoloration is a phenomenon where concrete loses its original color due to chemical changes in its compounds. Increase in volume of quartz-based aggregates and decomposition of limestone aggregates are examples of aggregate changes. Carbonation occurs when concrete compounds undergo chemical changes producing calcium carbonate, which reduces the alkalinity of concrete, causing corrosion of reinforcements. Spalling is a process in which parts of concrete are expelled from the solid concrete body. This happens due to the buildup of the pore pressure inside the concrete matrix (Persson, 2004).

Helal et al. (2010) reported that concrete partially loses its strength at a temperature of 392°F - 482°F (200°C - 250°C), but cracks occur at about 572°F (300°C) where concrete loses approximately 30% of its compressive strength, and the loss of strength continues with increase in temperature. This study also compared mechanical properties of SCC and VC at elevated temperature and concluded that residual strength of SCC after fire exposure was higher than that of VC. For gradual cooling, the compressive strength for SCC at 392°F (200°C) increased by 5.7% compared to its reference value. With increasing temperature, the compressive strength reduced but the reduction in SCC was less when compared to VC. At 752°F (400°C) and 1112°F (600°C) the reduction in compressive strength for SCC was 9.43% and 27.73%, respectively. Whereas for VC, the compressive strength at 392°F (200°C) initially increased

by 4.47%, but with increasing temperature of 752°F (400°C) and 1112°F (600°C), the compressive strength reduced by 16.15% and 49.32%, respectively. For sudden cooling, the reduction percentages were higher, and followed the same trend where percentage reduction for SCC was lesser when compared to VC. On comparing the split tensile strength, reductions for SCC were lesser than VC for gradual cooling and higher than VC for sudden cooling. Figure 2 and Figure 3 presents the results for compressive and split tensile strength from this study.

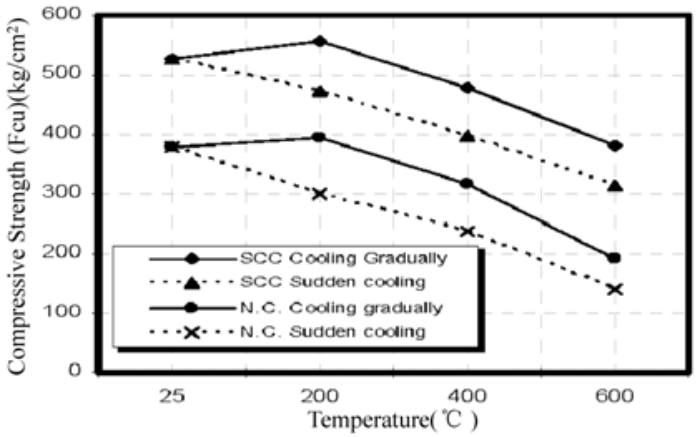

Figure 2: Relationship between temperature and ultimate compressive strength for concrete at 28 days (Helal et al., 2010)

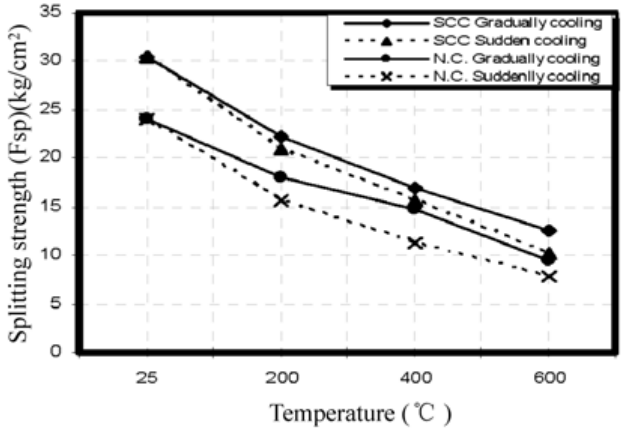

Figure 3: Relationship between temperature and splitting tensile strength for concrete at 28 days (Helal et al., 2010)

In his 2004 study, Persson explored self-consolidating concrete under fire and concluded that without PP fibers, SCC showed explosive spalling. Person hence posited that once spalling was avoided, both the concretes behaved similarly, the strength of SCC at higher temperatures

followed similar patterns of VC and strength decreased less when compared to high performance concrete HPC with temperature increase.

2.2 Fire Spalling in Self Consolidating Concrete

Spalling is a serious problem encountered by concrete at higher temperatures. Spalling results in separation of concrete mass from the whole matrix, causing reduction in the area of concrete that contributes towards the strength thereby significantly reducing the strength of concrete post fire exposure. Persson (2004) explained the spalling phenomenon as the result of buildup of pore water pressure and stated that when concrete is exposed to elevated temperatures, relative humidity (RH) of concrete increased with temperature resulting in the formation of fluid water. This water is transported towards the center of the specimen through voids where the space is limited. At a critical temperature of 705°F (374°C), this water is converted into steam, resulting in increased pressure/stresses within the concrete matrix. This sudden increase of pore pressure causes explosive spalling of the matrix. Persson (2004) concluded that fire spalling is dependent on the stresses in concrete, cement- powder ratio, and water-cement ratio.

Another study by Varona et al. (2018) stated that the dehydration of C-S-H gel and the portlandite generates water stream which provokes increase of the pore pressure, causing spalling. Also, thermal gradients and thermal incompatibility of the components of concrete mix with different thermal coefficients are the reasons for spalling to occur.

Numerous researchers (Ding et al., 2012; Varona et al., 2018; Li et al., 2020; Wu et al., 2020) suggest the use of microfibers, such as polypropylene and polyethylene, to restrict spalling in concrete. Yan et al. (2020) in his study with steel fibers (high melting point) and polypropylene fibers (low melting point) observed the microstructure changes of concrete using scanning electron microscopy (SEM) at high temperatures. The researchers concluded

that polypropylene fibers with a lower melting point are absorbed by the matrix at higher temperatures, creating interlacing voids. These voids assist in removal of pore and steam pressure developed in the matrix, and the concrete damage at higher temperatures was reduced.

Li et al. (2020) in his study reported that polyethylene fibers (PE) with a smaller coefficient of thermal expansion (10 x 10-5/°c) than PP (> 21 x 10-5/°c) create lower tensile stresses in the tangential direction along the fiber-matrix interface, and fewer cracks with smaller width are generated in the PE sample. Therefore, fiber voids formed by melted PE fibers do not adequately percolate or release vapor pressure. Furthermore, viscosity of PE fibers is several times greater than the viscosity of PP fibers. Therefore, the melted PE may block the micro cracks, and the water vapor cannot be released Typically, the melting point of polypropylene fiber is approximately 329°F - 392°F (165°C - 200°C); whereas the melting point of polyethylene fibers is about 293°F (145°C)Field emission scanning electron microscope (FESEM) images of steel, polypropylene and polyethylene fibers in the concrete matrix are shown in Figure 4, Figure 5 and Figure 6.

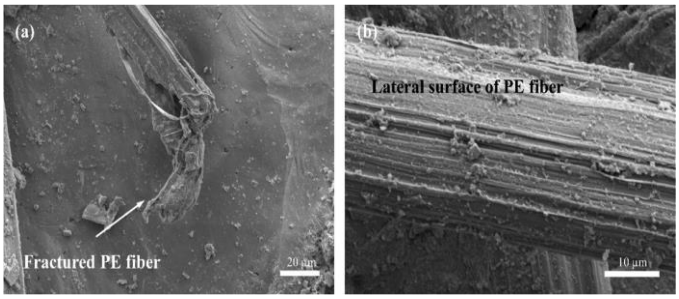

Figure 4: FESEM image of PE fiber on UHPFRC fracture surface (a) End of PE fiber (b) Lateral surface of PE fiber (Li et al., 2020)

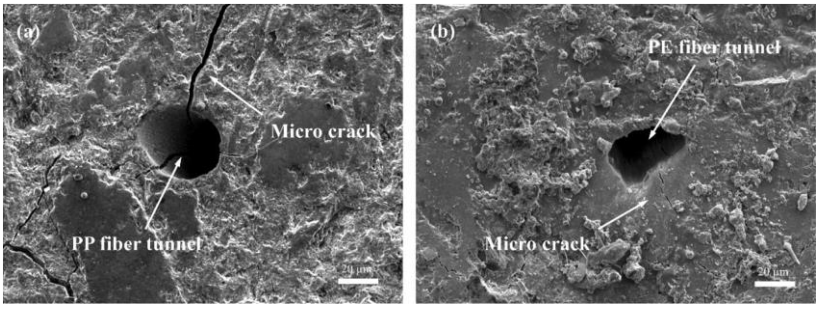

Figure 5: Cross section of UHPFRC samples with (a) PP and (b) PE fibers after exposure to 180 ℃ (Li et al., 2020)

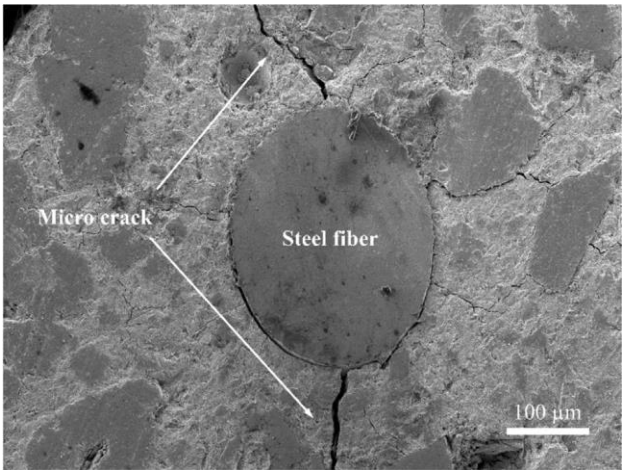

Figure 6: Cross section of UHPFRC with steel fiber after exposure to 300℃ (Li et al., 2020)

2.3 Steel Fiber Reinforced Concrete (SFRC) in Fire

Steel fibers are added in the concrete mix to enhance its tensile and flexural properties. Wu et al. (2020) stated that the relative compressive strength of SFRC linearly decreases with increasing temperature, and the rate of strength reduction may be affected by the replacement material. Furthermore, the steel fibers enhanced material strength at high temperatures and the degree of improvement depends upon the fiber dosage.

Zheng et al. (2012) explored compressive stress – strain relation for reactive powder concrete (RPC) with different volumes of steel fibers (1% SRPC1, 2% SRPC2, and 3% SRPC3) and subjected the fibers to elevated temperature. The researchers concluded that after being heated to same temperature, the compressive strength of SRPC3 and SRPC2 were roughly same and higher than SRPC1; and followed a similar trend with a temperature increase. When exposed to the temperature of approximately 572°F (300°C), RPC undergoes *high temperature curing*, which increases the cement hydration reaction. The compressive strength improved slightly compared to the original unheated specimen. After exposure to levels of heat between 572-1292°F (300-700°C), the internal damage to RPC increased gradually with the temperature, and the compressive strength reduced gradually. The corresponding strength loss

of SRPC2 and SRPC3 after 1292°F (700°C) was 87% and 85%, respectively, as shown in Figure 7.

In terms of peak strain, the above study reported that when the temperature is less than 932°F (500°C), the steel fiber content has little effect on the peak strain. However, when the temperature exceeds 932°F (500°C), peak strain increased along with increasing steel fiber content. Moreover, for various steel fiber contents, the development trend of peak strain was similar with the temperature increase. When the temperature is less than 572°F (300°C), the peak strain is approximately equal to the original unheated value, but when the temperature is in the range of 572°F-1112°F (300°C-600°C), the peak strain increased exponentially with the increasing temperature. However, when the temperature exceeds 1112°F (600°C), the weakened effect of steel fibers leads to the decline of RPC toughness; thus, the peak strain decreases linearly with the increasing temperature, as shown in Figure 8 .

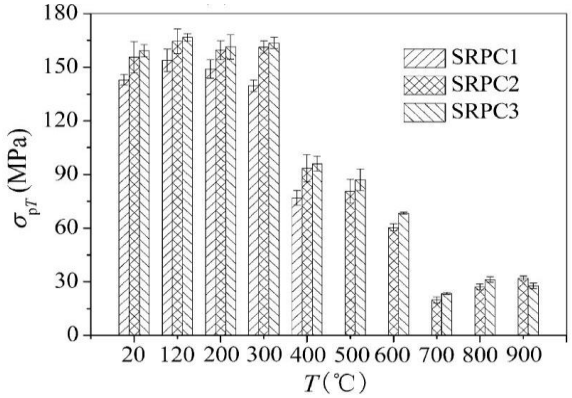

Figure 7: Relationship of compressive stress for steel fiber reinforced RPC with heating temperatures (Zheng et al., 2012)

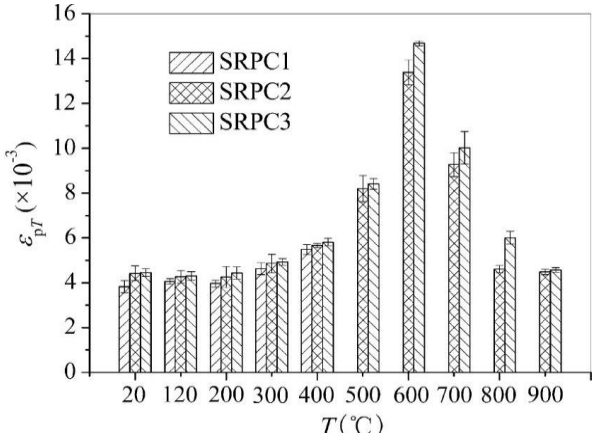

Figure 8: Relationship of peak strain for steel fiber reinforced RPC with heating temperatures (Zheng et al., 2012)

Ning et al. (2015) studied the effects of macro steel fibers on flexural behavior of reinforced SCC beams. Seven full-scale steel fiber reinforced self-consolidating concrete (SFRSCC) beams were tested with fiber content using reinforcing steel ratios as test variables. Ning et al. posited that the main difference between traditional SFRC and SFRSCC was the fiber content of SFRC was determined based on the post-cracking behavior of the composite. Nevertheless, for SFRSCC, the fiber content was determined based on the workability of the concrete as the workability of SFSRCC was damaged by the addition of steel fibers. The workability additionally decreased as fibers increased, as evident in Table 1. The cracking load was not significantly affected by the addition of fibers, but after cracking was observed, the addition of steel fibers greatly enhanced the flexural stiffness of the beam.

The authors observed that, with an increasing volume of fiber content, the ultimate and yielding load were effectively enhanced, and the midspan deflection corresponding to the loads decreased. For a fiber content of 50 lb./yd3 (30 kg/m3) and 84 lb./yd3 (50 kg/m3), the yielding load was increased by 19% and 34.5%, respectively, with respect to the control beam. For the same dosage rate of fibers, the ultimate load was enhanced by 11.4% and 18.8%, respectively, as seen in Table 2. The extent of improvement also depends on the type of fibers, shape, size, volume, and distribution of fibers in the mix. The fibers added to the mix must be evenly distributed to achieve uniform strength throughout the mix. The addition of steel fibers made concrete more ductile as the fibers reduced the crack width and mitigated the spread of micro-cracks due to the bridging effect.

Table 1: Fresh and mechanical properties of SFRSCC mixture (Ning et al., 2015)

Fiber contents (kg/m^3)	Slump flow		L-box			$f_{cu,28}$ (MPa)	$f_{c}^{'}{}_{,28}$ (MPa)
	d_m(mm)	T_{500}(s)	H_2/H_1	T_{200}(s)	T_{400}(s)		
0	780	3.1	0.91	2.2	5.1	65.3	52.2
30	740	3.4	0.87	2.7	6.4	67.0	53.6
50	700	4.4	0.81	4.9	9.7	66.8	53.4

Table 2: Failure mode and test results at different loading stages (Ning et al., 2015)

Specimen Notation	f_{cu} (Mpa)	$f_{c}^{'}$ (MPa)	At cracking		At yielding		At ultimate		Failure mode
			P_{cr} (kN)	δ_{cr} (mm)	P_y (kN)	δ_y (mm)	P_u (kN)	δ_u (mm)	
BS-A-PC	65.3	52.2	34	0.45	116	5.3	167	43.4	Flexural
BS-A-SF30	67.0	53.6	35	0.53	138	4.9	186	40.4	Flexural
BS-A-SF50	66.8	53.4	37	0.58	156	5.2	198	30.7	Flexural
BS-B-PC	75.6	60.5	39	0.58	147	5.8	195	42.4	Flexural
BS-B-SF30	77.4	61.9	41	0.51	171	4.9	206	38.5	Flexural
BS-B-SF50	68.4	54.7	37	0.41	183	5.5	215	33.7	Flexural
BS-C-PC	63.3	50.6	39	0.57	186	6.2	227	37.7	Flexural

2.4 Polypropylene Fiber Reinforced Concrete in Fire

Ahmed et al. (2006) states that polypropylene fibers in the concrete mix limit plastic shrinkage, cracks, and fire spalling. The fibers melt at about 320°F (160°C) in the concrete mix, causing voids which lead to the expulsion of water and steam vapors from the concrete matrix. Therefore, this process reduces the pressure within the matrix. Polypropylene fibers are also used in very small amounts as they impact the concrete mix's strength. However, polypropylene fibers used in excess have a negative effect on the concrete strength. The addition of polypropylene fibers at low dosage of about 0.35% increased the compressive strength by 5%. When the dosage was increased to 0.55%, the compressive strength decreased by 3%. In terms of tensile strength, the addition of fibers proved to be beneficial. The tensile strength increased by 65-70% for a dosage of up to 0.40% of fibers by volume, after which the tensile strength decreased, affirming the effect of using an excessive amount of fibers.

The authors observed that flexural strength behavior of concrete was similar to that of tensile strength; however, the range of fiber dosage was limited to 0.25% to obtain the best results. For a dosage of 0.20%, the flexural strength was enhanced to 80%, resulting in a decrease in strength due to the increasing fiber content. The researchers also report that using 0.35% of polypropylene fibers by volume reduced the plastic shrinkage cracks to a great extent when compared to levels of shrinkage cracks when manufacturing concrete without fibers. Moreover, shrinkage cracking was reduced by 83-85% at room temperature by adding fibers up to 0.35 – 0.55% The above comparisons are shown in Figure 9.

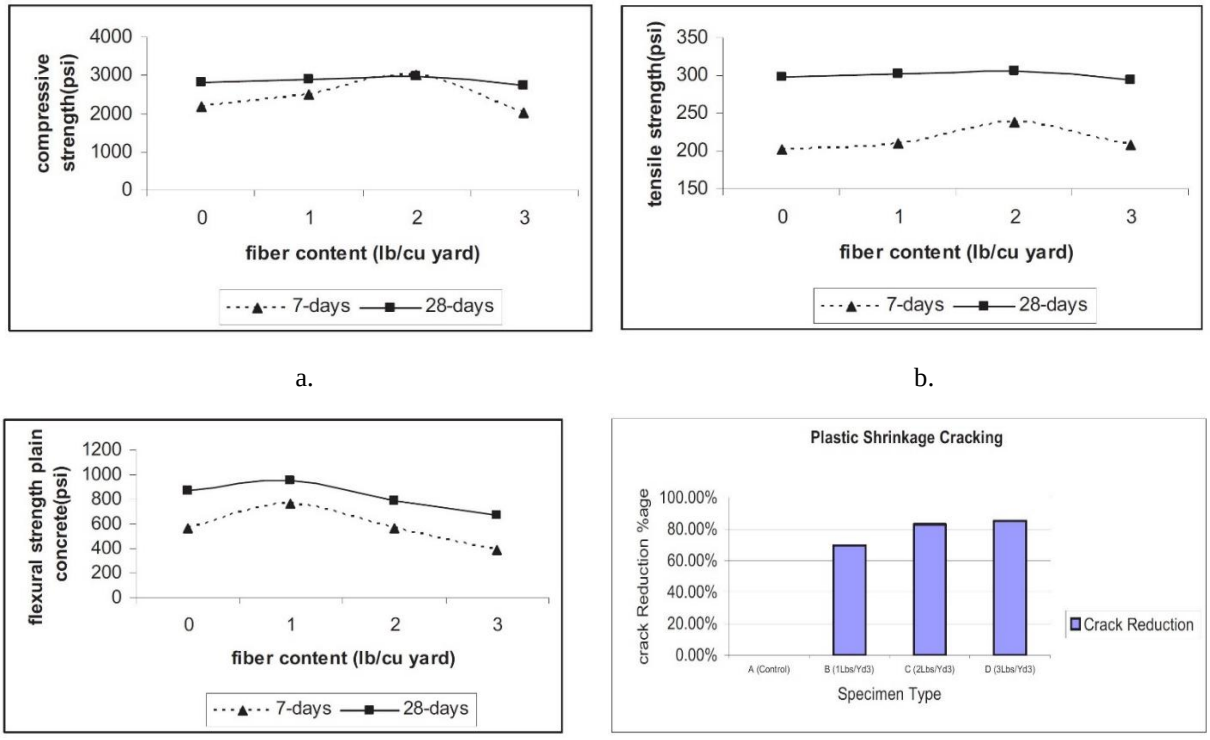

Figure 9: Strength parameters vs fiber content: a) Compressive strength; b) Tensile strength; c) Flexural strength; d) Percentage reduction in plastic shrinkage (Ahmed et al., 2006)

2.5 Hybrid Fiber Reinforced Concrete (HFRC) in Fire

The performance of Fiber Reinforced Concrete (FRC) under high temperatures is affected by various factors, including the use of replacement materials and addition of reinforcing fibers. Based on various functions in concrete fire resistance, reinforcing fibers can generally be

divided into two groups, macro-fibers, and micro-fibers. The macro-fibers group, which consists of steel fiber, carbon fiber, and basalt fibers, typically exhibits appropriate mechanical properties at room temperature and thermal stability at higher temperatures. The microfibers group includes PP fiber, PVA fiber, and PE fiber, all of which have a low melting point and melt at high temperatures while protecting the microstructure of concrete by reducing inner vapor pressure (Wu et al., 2020).

Varona et al. (2018) stated that HFRC, including steel fibers with a higher aspect ratio, gave better residual compressive strength up to 1202°F (650°C) than the SFRC**,** even when the SFRC had twice the fiber content by volume fraction than HFRC. This result supports the hypothesis of synergy of steel and polypropylene fibers in fire action. The researchers concludes that the effect of high temperatures on residual mechanical properties of hybrid fiber-reinforced concrete was less severe than in steel fiber-reinforced concrete. The researchers also discuss the effect of aspect ratio of steel fibers. A high aspect ratio of steel fibers is more efficient at ambient temperature; however, at high temperatures, steel fibers did not provide the same degree of ductility.

Ding et al. (2012) compared the different variants of self-consolidated high-performance concrete (SCHPC), i.e., steel fiber-reinforced SCHPC (SF40 and SF55), polypropylene fiber-reinforced SCHPC (PP2), and hybrid fiber-reinforced SCHPC (HF403 and HF552). For each of the mixes, the residual compressive strengths were reported as seen in Figure 10. SCHPC without fiber showed the greatest loss in strength when exposed to the respective temperatures, 300°C (572°F), 600°C (1112°F), and 900°C (1652°F). Furthermore, loss in compressive strength was 17%, 67% and 94%, respectively, compared to the original strength before heating. For SCHPC (PP2), the relative loss in strength was lower when compared to the SCHPC without fibers. For a temperature exposure of 300°C (572°F) and 900°C (1652°F), the respective strength losses were 14% and 89%. Among the SF 40 and SF55

fibers, SF 55 showed less reduction in compressive strength when exposed to higher temperatures due to the higher dosage rate of SF55. When exposed to temperature of about 300°C (572°F), 600°C (1112°F), and 900°C (1652°F), the respective loss in compressive stress for SF55 was 8%, 59%, and 91%, respectively whereas for SF40, the losses were 16%, 63%, and 91%, respectively. When HF403 and HF552 were exposed to 600°C (1112°F), they retained about 43% of their original compressive strength while at 1652°F (900°C) the retention was 11%.

These comparisons underscore the effect of different fiber reinforcement types on the residual compressive strength where hybrid fiber reinforcement supersedes the mono fiber reinforcement and concrete without fibers suffered more loss comparatively. These comparisons also emphasize the effective synergy of steel and polypropylene fibers in fire hazards. In terms of workability, Ding et al. (2012) reported that the introduction of fibers reduced the workability of the concrete, and as the fiber content increased, so did the reduction. PP fibers also had a more significant effect on workability than the steel fibers. Table 3 shows the difference in workability for different types and dosages of the fibers.

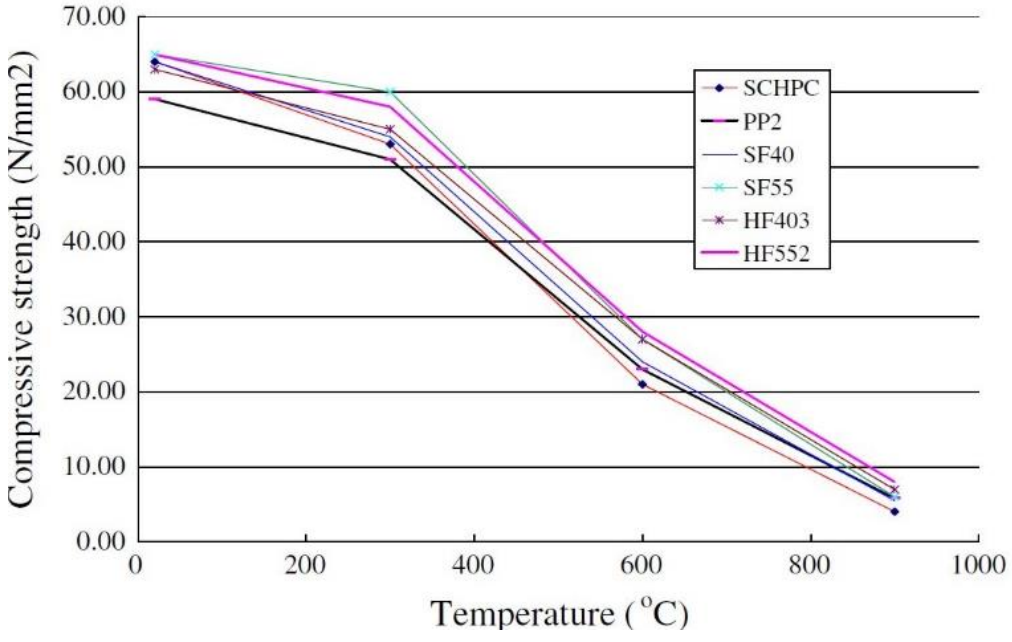

Figure 10: Comparison of compressive strength after various temperatures (Ding et al., 2012)

Table 3: Test results of workability (Ding et al., 2012)

Mixtures	SCHPC	PP2	SF40	SF55	HF403	HF552
PP fibre content (kg/m^3)	–	2	–	–	3	2
Steel fibre content (kg/m^3)	–	–	40	55	40	55
Slump flow (mm)	678	632	662	646	604	608
J-Ring, J_{sf} (mm)	650	585	610	590	545	540
J-Ring, L_J (mm)	5	20	10	15	35	30
U-box (h_1–h_2, mm)	5	25	23	27	32	30

2.6 Glass Pozzolan as Cement Replacement

Kaminsky et al. (2020) in his report states that the construction industry is persistently looking for new versions of advantageous cementitious materials (SCMs) to substitute the Portland cement. Fly ash, slag cement, and silica fume are utilized in current substantial combinations. Extensive research and testing have shown that few sorts of ground glass will perform as well as a pozzolan in concrete. Unfortunately, glass creation is a significant source of ozone harming substances. While reusing glass can decrease the ecological effect, 8.4 million tons (7.6 million tonnes) of holder glass ends up in landfills every year in the U.S. (roughly triple the sum that is reused). A preliminary, third-party life-cycle evaluation of one such ground-glass pozzolan (GGP) producers yield shows that the Global Warming Potential (GWP) sway for 1 ton (0.9 tonne) of GGP produced is 123 lb. (56 kg) of CO_2. For comparison, the typical U.S. industry GWP for Portland cement is 2293 lb. (1040 kg) of CO_2. Accordingly, the GWP determined for a concrete project in New York city with 50% cement replacement using GGP would be about 40% less than the GWP for concrete mixture with cement only. ASTM C1866/C1866M (20) requires that at least 95% of the glass powder passes a 325-mesh wet sieve (particles smaller than 45 microns). When processing to 95% passing a 45-micron sieve, there is no danger of from these leftover particles as they are not sufficiently big enough to cause ASR as this is a surface area dependent phenomenon.

In Tapia's (2020) research, it established comparison between plain concrete and concrete with 20% cement replacement using glass pozzolan and reported that the average compressive strength tested as per ASTM C39 (2018) reported a 3% increase at 90 days for concrete with glass pozzolan when compared to the plain concrete as shown in Figure 13. In terms of flexural strength at room temperature, Tapia also reported that beams with glass pozzolan showed higher flexural strength by a margin of 10% when compared to beams without glass pozzolan as shown in Figure 11. None of these beams had steel reinforcement; to establish proper comparison between the glass pozzolan concrete and plain concrete.

Residual flexural strength of these beams after a 30-minute heat exposure of 1550°F (843°C) as per the ASTM E119 (2019) fire testing standards, reported a loss of 93% for beams with glass pozzolan, whereas beams with plain concrete observed 95% loss in their flexural strength as shown in Figure 12. The plain concrete samples exposed to one hour heat exposure of 1700°F (927°C) failed even before being tested for the residual strength. On the other hand, the beams with glass pozzolan reported some residual flexural strength after one hour fire exposure. These comparisons show the benefits of adding glass pozzolan on the mechanical properties of the concrete. Tapia concluded that beams with glass pozzolan reported more ductile behavior after fire exposure when compared to beams at room temperature.

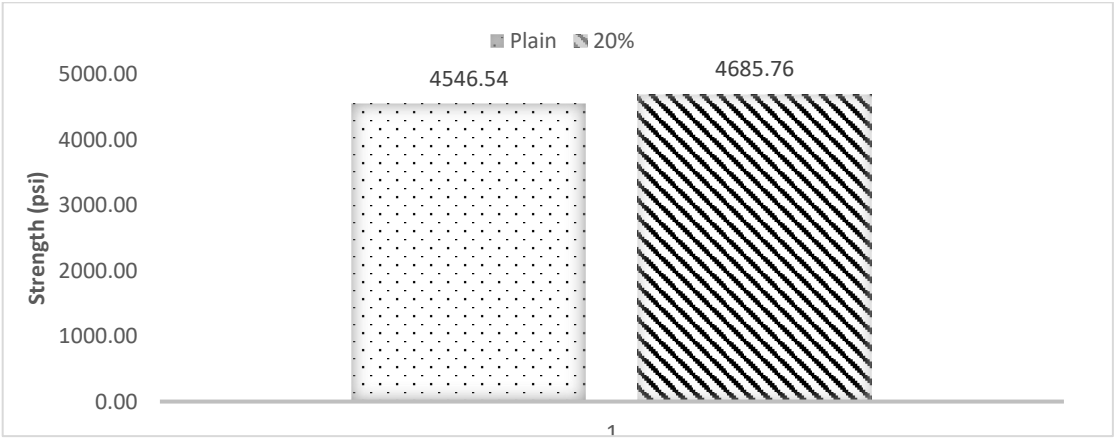

Figure 11: Average compressive strength of concrete mixtures at room temperature (Tapia., 2020)

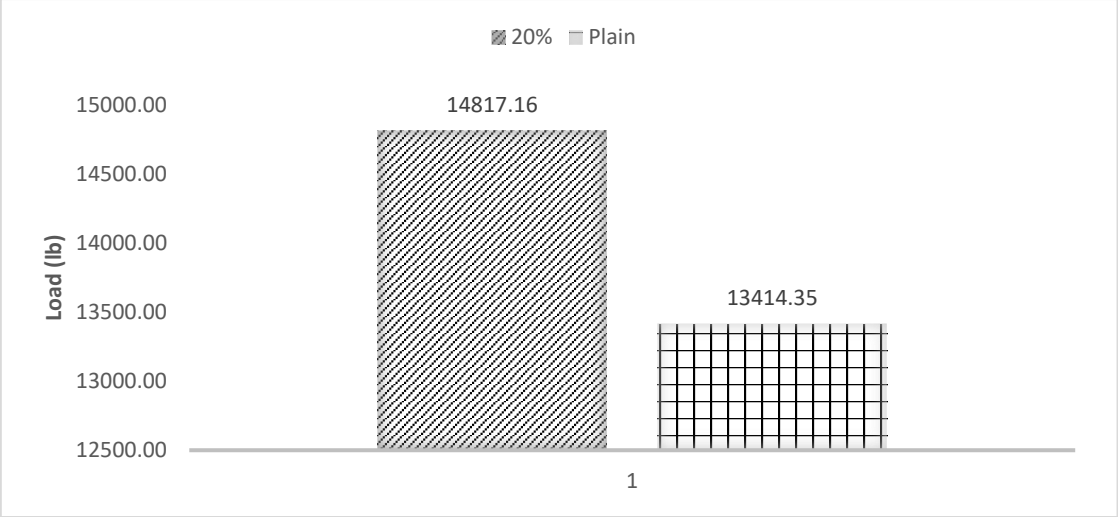

Figure 12: Average flexural load for beams at room temperature (Tapia., 2020)

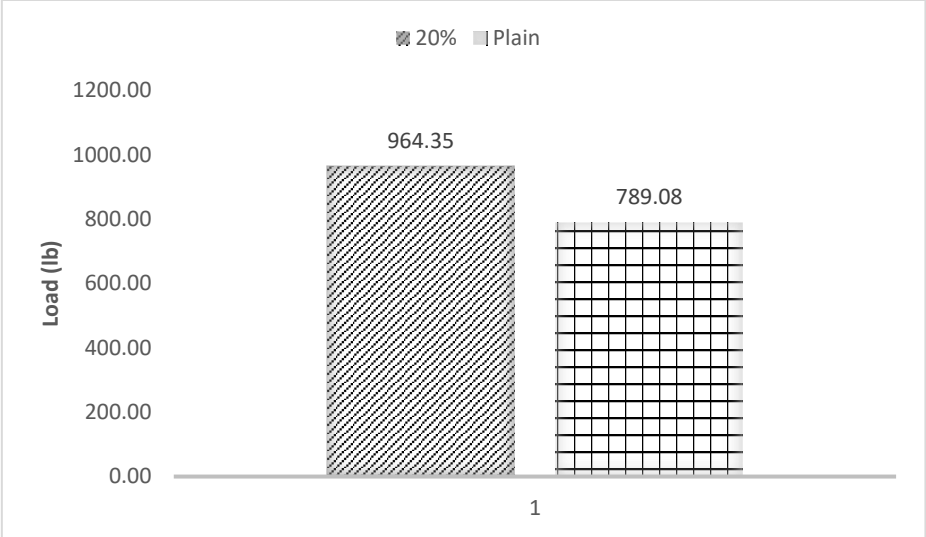

Figure 13: Average flexural load for beams after 30 mins heat exposure (Tapia., 2020)

Chapter 3

Experimental Design & Sample Preparation

3.1 Experimental Procedure

To successfully study the effects of hybrid fibers and cement replacement, samples were cast and tested. Four different mixes were planned; the variables of the mixes were the cementitious materials and hybrid fibers. The dosage of hybrid fibers was kept constant for all four mixes, and a mix of cementitious materials and the hybrid fibers was created. The first mix was cast using only the Portland cement and was designated the control SCC mix. The second mix included VCAS glass pozzolan as a replacement for 20% of the cement. This was to study the behavior of glass pozzolan used for cement replacement under fire action. Two additional mixes were cast in which the hybrid fibers were introduced to the initial two mixes as the third variable. The four mixes and their design parameters are shown in Table 4. The four different mixes are:

- R-SCC: Regular SCC (control).
- G-SCC: SCC with 20% VCAS glass pozzolan as cement replacement.
- F-SCC: SCC with steel and polypropylene as hybrid fibers.
- FG-SCC: SCC with steel and polypropylene as hybrid fibers and 20% glass pozzolan as cement replacement.

Each mix design had three beams that were 36 in. x 8 in. x 8 in. (0.914 m x 0.20 m x 0.20 m) and six cylinders that were 4 in. (0.10 m) in diameter by 8 in. (0.20 m) in height. In total, there were 12 beams and 24 cylinders. To study the effect of hybrid fibers in full capacity, no rebars were used as reinforcements. For the purposes of the study, steel fibers were considered as the only reinforcement available to the specimens. The plan and elevation for the specimens are shown in Figure 14.

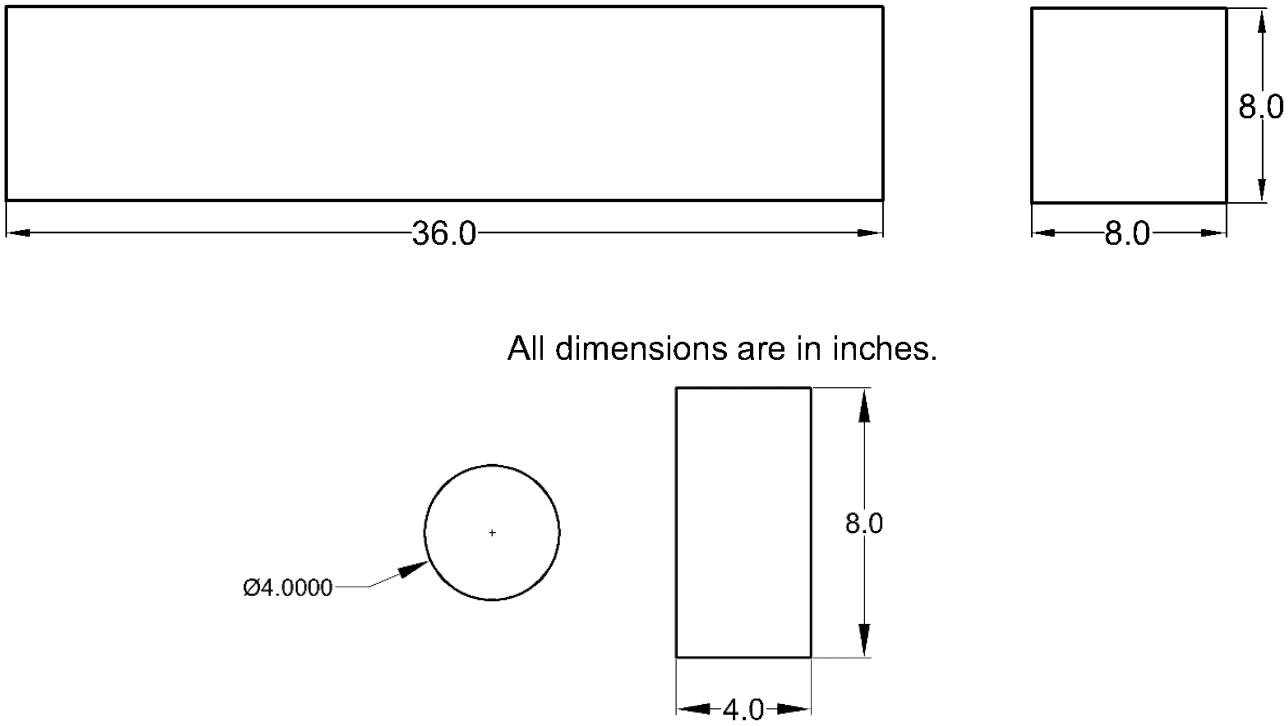

Figure 14: Plan and Elevation of specimens

Table 4: Mix design parameters

Mix Designation	**Cement Content (%)**	**Glass Pozzolan Content (%)**	**Steel Fibers Content (lb./yd^3)**	**Polypropylene Fibers Content (lb./yd^3)**	**No. of Specimens**	**Remark**
R-SCC	100	0	0	0	Beams-3 Cylinders-6	Control
G-SCC	80	20	0	0		
F-SCC	100	0	3.5	1.5		
FG-SCC	80	20	3.5	1.5		

3.2 Raw Materials Used in the SCC Design Mix

3.2.1 Steel Fibers

The steel fibers used in this research were provided by Euclid Chemicals. A low carbon, cold-drawn, and hooked-end steel wire fiber, PSI Steel Fiber C6560, was used. The fiber is

designed to provide concrete with temperature and shrinkage crack control, enhanced flexural reinforcement, improved shear strength, and increase the crack resistance of concrete. The PSI steel fiber C6560 complies with ASTM C1116 (2015) and ASTM A820 (2011). For industrial purposes, the typical dosage rate for these fibers were 12 – 100 lbs./yd^3 (7 – 60 kg/m^3) or higher. A smaller dosage, however, was used for the present study. The recommended dosage for a SCC mix was 3.5 – 4.5 lbs./yd^3 (2 – 2.7 kg/m^3) (Euclid chemicals, 2021). The adopted dosage used in the present study is 3.5 lbs./yd^3 (2 kg/m^3). The steel fibers are shown in Figure 16, and their physical properties are listed in Table 5.

Table 5: Physical properties of PSI Steel fibers C6560

Parameter	Specification
Material	Low carbon cold drawn steel wire
Deformation	Hooked end
Length	2.375 in. (60 mm)
Aspect ratio	65
Tensile strength	160 ksi (>1100 MPa)
Color	Bright clean wire

3.2.2 Polypropylene Fibers

Polypropylene microfibers from Euclid chemicals were used in the present study. The fibers are monofilament microfibers that comply with ASTM C 1116 (2015) and are specifically designed to help mitigate the formation of plastic shrinkage cracking in concrete. The fibers meet the necessary standards of the International Code Council (ICC) Acceptance Criteria AC32 for synthetic fibers. Among the various available lengths of 0.25 in. (6.35 mm), 0.50 in. (12.7 mm), and 0.75 in. (19.05 mm), the fibers were opted with multi blend lengths which consist of portions of all the available lengths. The typical dosage rate of the fibers is 1 – 3 lbs./yd^3 (0.45 – 1.36 kg/m^3) (Euclid chemicals, 2021). The dosage rate used in the mix

design is 1.5 lbs./yd^3 (0.90 kg/m^3). The physical properties of PSI Fiberstrand 100 are listed in Table 6. The fibers are as shown in Figure 16.

Table 6: Technical information on PSI Fiberstrand 100

Parameter	Specification
Material	100% virgin monofilament polypropylene
Specific Gravity	0.91
Length	Multi blend (ML)
Melting point	320°F (160°C)
Electrical and thermal conductivity	Low
Water absorption	Negligible
Acid and alkali resistance	Excellent
Color	White

3.2.3 Glass Pozzolan

Vitreous Calcium-Alumino-Silicate (VCAS) 140 glass pozzolan is made from crushed E-glass. A pozzolan is a material that is only cementitious when mixed with cement powder and water. VCAS reacts with lime (CaOH) and forms additional cement binder (Calcium-Alumino-Silicate hydrate). E-glass is low in alkali and is very effective in mitigating Alkali Silica Reaction (ASR), a major concerns of using glass pozzolans as cement replacements (Vitro Minerals, 2020). This specific type of pozzolan meets the ASTM C1866 (2020) specifications for glass pozzolans. The VCAS glass pozzolan grades exhibit 10% lower water demand when compared to silica fume or metakaolin and can be used for cement replacement up to 40%.

In the present study, a replacement rate of 20% is used. VCAS 140 has particle size of 12 microns, as shown in Figure 15. Approximately 94% of VCAS' composition is formed from calcium, aluminum, and silica, (see Table 7). Table 8 shows physical properties for VCAS 140 glass pozzolan.

Table 7: Chemical composition and weight percentage for VCAS 140 Glass Pozzolan

Element Oxide	Weight Percent
SiO_2	59.9
Al_2O_3	12.5
Fe_2O_3	0.37
CaO	21.4
MgO	2.91
Na_2O	0.77
K_2O	0.06
SO_3	<0.1
Loss on Ignition, LOI	<0.1
Organic Content, Max %	0

Figure 15: VCAS 140 glass pozzolan

Table 8: Physical properties of VCAS 140 Glass Pozzolan

Parameter	Specification
Specific Gravity	2.6
Bulk Density, Loose lbs./ft^3	50-55
Passing No. 325 Mesh, %	95
Median particle size, d50, µm	12
Pozzolanic Strength Index, %	104
Brightness, %	82-85
Melting Point, °C (°F)	1200 (2192)
Hardness, Mohs	5.5

3.2.4 Superplasticizer

Plastol SPC, a polycarboxylate based high range water reducing admixture (HRWRA) that allows concrete to be developed with very low water-cement ratios was used. This superplasticizer produces self-consolidating concrete with low doses and can obtain water reduction up to 45% and is known to produce high early and ultimate strength concrete. Plastol SPC complies with the requirements of ASTM C 494 (2019), type A and F admixtures, and AASHTO M 194 (2006). The product data sheet recommends a dosage rates are 3 to 12 oz per 100 lbs. (200 to 780 mL per 100 kg) of cementitious material (Euclid chemicals, 2021). However, the dosage rates vary depending upon the characteristics of materials being used in the mix; and for that reason, the datasheet advises to carry out a few trials using SPC before finalizing the dosage. As for usage, SPC can be directly added to the water or directly to the freshly batched concrete. The datasheet also recommends mixing the raw materials for at least five minutes after the addition of the Plastol SPC. The dosage used for this project was 8 oz per 100 lbs. (236 mL per 100 kg) of cementitious material.

3.3 Concrete Mix Design

The concrete mix design was performed per the ACI 232.7R (2007) using the ACI Volumetric Method (2009). Since the concrete type was SCC, the target slump was set initially. For the target slump, the range for cement content was obtained from the ACI guide. The ACI guide also provided recommendations for the percentage of course and fine aggregates as well as a range for the w/c ratio between 0.32 – 0.45. Based on these recommendations in conjunction with the volumetric design methods, volume for coarse and fine aggregates were obtained. Table 9 Table 10 are excerpts from the ACI guide that highlights the approximate percentage of proportions in the SCC mix. Figure 16 shows the raw materials used in the concrete mix.

a.

b.

c.

d.

Figure 16: Raw materials used in design mix: a) Coarse aggregates (gravel); b) Fine aggregates (sand); c) Steel fibers; d) Polypropylene fibers

Table 9: Suggested powder content for target slump from ACI 232.7R (2007)

	Slump Flow of < 22 in. (<550 mm)	**Slump Flow of 22 - 26 in. (550 – 650 mm)**	**Slump Flow of > 26 in. (>650 mm)**
Powder Content lb./yd^3 (kg/m^3)	600 to 650 (355 to 385)	650 to 750 (385 to 445)	750+ (458+)

Using 4 ft. x 8 ft. (1.22 m x 2.44 m) standard OSB boards and 2 in. x 4 in. (0.051 m x 0.10 m) lumber, the required formworks were developed. The boards and lumbers were cut to the required sizes and then screwed together to develop the formwork for the samples as shown in Figure 17.

Figure 17: Beam formwork

Table 10: SCC proportioning summary from ACI 232.7R (2007)

Summary of SCC proportioning trial mixtures parameters	
Absolute volume of coarse aggregates	28 to 32% (>1/2 in. (12mm) nominal maximum size)
Paste fraction (calculated on volume)	34 to 40% (total mixture volume)
Mortar fraction (calculated on volume)	68 to 72% (total mixture volume)
Typical w/cm	0.32 to 0.45
Typical cement (powder content)	650 to 800 lb./yd^3 (386 to 475 kg/m^3)

3.3.1 Trial Mixes

Based on ACI's (2007) recommendations, certain assumptions were made to obtain a successful mix design and are discussed in this section. The target slump was set to 22 in. (0.56 m), and from the recommended range, powder content was assumed to be 600 lbs./yd^3 (356 kg/m^3). Mix FG-SCC was chosen as the trial mix as it contained both fibers and glass pozzolan, which made it the most critical mix among the other mixes. Maximum coarse aggregate was set to 1 in. (25.4 mm), and the absolute volume of coarse aggregates was assumed as 30%. From the recommended mortar fraction, the percentage of fine aggregates was found equal to

32%. The water content was fixed as 0.45 initially. The volume of trial mixes was fixed at 0.02 yd3 (0.0153 m3) for the purposes of the slump test.

A mix was designed based on the above assumptions, and certain trials were planned by varying the fiber dosage and cement content. In the initial stages of the trials, the mix was overly hard and dry, and it hardly flowed (Figure 18: a). The microfibers are believed to affect the workability of the mix (Ding et al., 2012), and the same phenomenon was evident in the trials. These effects of fibers on workability were more than expected and trial slump obtained was in the range of 5 in. (0.13 m). Based on this, the microfiber content in the mix was reduced and, in an attempt to increase the water content, the cement content was increased to 700 lbs./yd3 (415 kg/m3). With these considerations, several other trials were carried out, and these changes made the slump slightly better; however, the flow obtained was still not sufficient. The flow obtained was in the range of 8.5 in. (0.22 m), as shown in Figure 18: b.

After several failed trials to obtain the target slump, it was decided to use superplasticizers in the mix design. Further trials were performed using the superplasticizer, and for a dosage of 10 oz per 100 lbs. of cementitious material, a slurry mix with slump flow of 29.5 in. (0.75 m) was obtained, which resulted in bleeding concrete, as shown in Figure 18: c. Two more trials with a reduced dosage of superplasticizers and w/c ratio were executed, and for a dosage of 8 oz per 100 lb. of cementitious material and w/c = 4.0, a concrete mix with slump flow of 22.5 in. (0.57 m) was obtained as shown in Figure 18: d. The mix design was subsequently finalized.

A trial beam as shown in Figure 19, and two cylinders were also cast for the finalized mix design. A detailed mix design based on the final successful trial is presented in *Appendix A.* Table 11 represents the quantities required to cast the trial samples whereas Table 12 presents the quantities of materials used in different trials.

a.

b.

c.

d.

Figure 18: Slump test results for Trials: a) Trial 1; b) Trial 6; c) Trial 12; d) Trial 16

Figure 19: Trial beam

Table 11: Quantities required to cast trial samples

Materials	Quantities required for a trial volume of 0.090 CY (lb.)
Cement	46.8
Glass pozzolan	11.7
C.A	77.76
F. A	120.6
Steel fibers	0.315
Polypropylene fibers	0.135
Water	23.4
Plastol SPC	0.2925

Table 12: Materials used for different trials

Materials	Trial #1	Trial #6	Trial #12	Trial #16
Cement (lb.)	9.60	11.20	10.40	10.40
Glass pozzolan (lb.)	2.40	2.80	2.60	2.60
C.A (lb.)	17.28	17.28	17.28	17.28
F. A (lb.)	26.80	26.80	26.80	26.80
Steel fibers (lb.)	0.090	0.080	0.070	0.070
Polypropylene fibers (lb.)	0.060	0.050	0.030	0.010
Water (lb.)	4.80	6.30	5.46	5.2
Plastol SPC (lb.)	NA	NA	0.0375	0.0325

3.4 Sample Preparation

For final samples, thermocouples were embedded into the specimens to be fire treated during casting, i.e., eight of the twelve samples. To accurately measure the beams' temperature during fire treatment, the thermocouples were fixed at the midsection and mid height of the beam. A small hole was drilled at the desired location into the formwork, and a thermocouple was inserted for a depth of four in. into the beam, as shown in Figure 20. Once the thermocouple was fixed, the hole was sealed thoroughly to make sure no loss of moisture occurs once the beam was cast. Using a sealant, the samples were also sealed at the edges to prevent moisture

loss. A release agent was then applied to the samples to ensure the hardened concrete did not adhere to the formwork surfaces in contact.

a. b.

Figure 20: Set up of thermocouple in the formwork: a) Fixed thermocouple; b) Close shot

3.5 Casting of Final Samples

Based on the test results from the trial samples, the trial mix finalized was used to cast 12 beams and 24 cylinders, constituting four different mixes, at the Civil Engineering Laboratory Building (CELB) at the University of Texas at Arlington (UTA). An available mixer in the laboratory with mixing capacity of nine cubic feet was used to properly mix the concrete, as shown in Figure 21. To avoid overloading of the drum mixer, each mix was divided into two separate batches. The two batches were proportioned as such that the first batch would be sufficient to cast one beam and six cylinders while the second batch would be enough to cast the remaining two beams. All four mixes were cast in eight different batches. Table 13 represents the total quantities required for 1 yd^3 (0.76 m^3) of concrete volume. The quantities required for each mix design are shown in Table 14. Figure 22 presents some of the images from the casting day at the CELB, and Figure 23 presents the final casted samples. To ensure thorough mixing of all materials--including hybrid fibers, glass pozzolans and admixture--a

detailed procedure was followed during casting. The procedure is as follows:

1.) Initially, the drum was rotated with some water inside it to wet the inner perimeter of the drum. Then the water was discarded.
2.) Fine and coarse aggregates were added to the drum along with hybrid fibers (if necessary) and mixed for a minute to ensure even distribution of hybrid fibers in the mix. One-fourth of the required water was added to the running drum and was mixed for another minute.
3.) Next, one-third of the cement and glass pozzolan (if necessary) were added and then mixed for a minute. Then again one-fourth of water was added to the drum and mixed for another minute. This step was repeated two more times until the full quantity of cement and glass pozzolans were emptied into the drum.
4.) After all the materials were added, the drum was mixed for an additional three minutes to maintain homogeneity of the mix.

Figure 21: Drum mixer used for mixing concrete

Table 13: Quantities required for 1 CY of concrete

Materials	**Quantities required for a volume of 1 CY (lb.)**
Cement	520
Glass pozzolan	130
C.A	864
F. A	1340
Steel fibers	3.5
Polypropylene fibers	1.5
Water	260
Plastol SPC	3.25

a.

b.

c.

d.

e.

Figure 22: Images from casting day: a) Measured raw materials; b) Raw materials added to the drum mixer; c) Glass pozzolan added to the drum mixer; d) Mixing of concrete; e) Final concrete after mixing

Table 14: Quantities required for each mix for 0.25 CY (0.19 m^3) of concrete

Constituent	**R-SCC**	**G-SCC**	**F-SCC**	**FG-SCC**
Cement (lb.)	162.5	130	162.5	130
Fine Agg. (lb.)	335	335	335	335
Coarse Agg. (lb.)	216	216	216	216
Water (lb.)	65	65	65	65
Glass Pozzolan (lb.)	NA	32.5	NA	32.5
Plastol SPC (lb.)	0.8125	0.8125	0.8125	0.8125
Steel Fibers (lb.)	NA	NA	0.875	0.875
Polypropylene Fibers (lb.)	NA	NA	0.375	0.375

a.

b.

c.

Figure 23: Final samples casted: a) Cylinders; b) Beams without hybrid fibers; c) Beams with hybrid fibers

Chapter 4

Test Procedures

4.1 Fire Test

4.1.1 Fire Conditioning

Once the trial sample was cast and cured for 28 days in an open environment outside the CELB, it was subjected to fire conditioning to limit the relative humidity (RH) of the specimen under 74% before fire treatment. The RH was limited to prevent the excessive spalling of the specimen within the furnace, and to avoid any damage to the instrument as the percentage of the water content is higher in SCC. The trial sample was demolded from the formwork, cleaned for any impurities, and then dried in the furnace as per the following procedure:

1.) The temperature of the furnace was set to 150°F - 175°F (65°C - 80°C) and the trial sample was left in the furnace for the initial 48 hours.
2.) For the next 48 hours, the furnace temperature was set to 200°F (93°C).
3.) After the 48-hour period, the temperature was raised to 300°F (149°C) for the next 24 hours.
4.) Finally, the furnace temperature was returned to ambient temperature over an eight hour-period at a rate of decrease of 30°F (16.6°C) per hour.

After the drying procedure was completed, the specimen was set aside in the lab and allowed to cool for a period of 24 hours. The specimen was then tested for RH content as per the ASTM F2170 (2011). As per the procedure, the beam's top surface was drilled to a depth of 3.2 in. (0.081 m) (40% of overall depth i.e., 8 in. (0.20 m)). The diameter of the hole was 0.75 in. (0.019 m). The hole was then cleaned of all dirt and residues using suction, and then a RH sensor was inserted and sealed into the drilled hole and left for 24 hours for calibration, as shown in Figure 24. The RH readings were subsequently taken after a calibration period of 24

hours. After the procedure, the RH content obtained for trial sample was 95% RH at 79°F (26°C), as shown in Figure 24. The suggested procedure was for normally vibrated concrete and did not seem to be effective for SCC. As the reduction in RH obtained was only 5%, no fire conditioning was performed for actual samples.

a.

b.

c.

Figure 24: Insitu RH test: a.) Installing the sensor; b.) Complete set up for calibration; c.) RH obtained

4.1.2 Fire Treatment

Once the 28-day curing period was complete, the final specimens were heat-treated as per the ASTM E119 (2019) standard for fire testing. This specification is basically a time versus temperature curve specifying the temperature that the specimen should have attained for a

given time. The ASTM E119 curve is as shown in Figure 25. The breakdown of this curve for an hour is shown in Table 15.

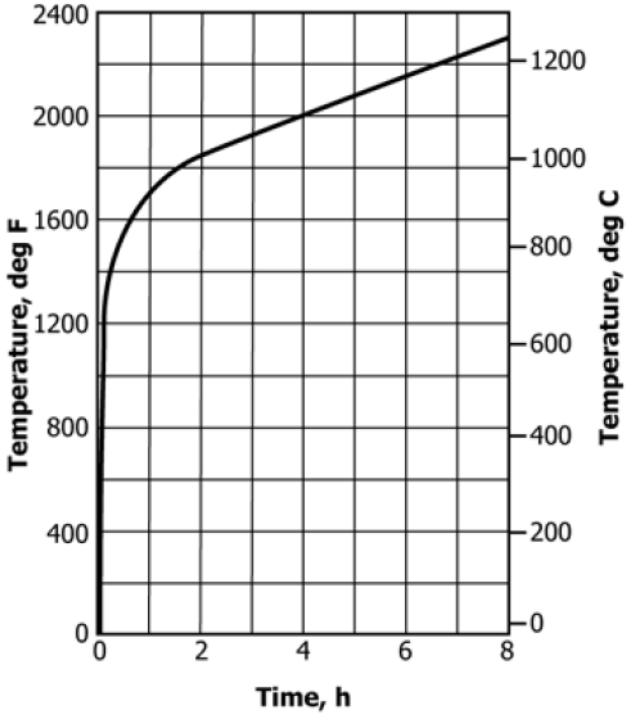

Figure 25: ASTM E 119 (2019) Fire testing curve

Table 15: Breakdown of time vs temperature curve

ASTM E119 (19) Fire testing standards for 1 hr.	
Time reached (min.)	**Temperature to be attained (°F (°C))**
5	1000 (538)
10	1300 (704)
15	1399 (760)
30	1550 (843)
45	1638 (892)
60	1700 (927)

From Table 15, when the testing time reaches 30 and 60 minutes, the furnace should have attained a temperature of 1550°F (843°C) and 1700°F (927°C), respectively. An electric furnace at the CELB was used for fire treatment. The furnace was programmed to follow the specified temperature curve, and the data from the above table served as an input to program the furnace. Once the fire test begins, the furnace aimed at reaching these specified

temperatures at the specified time intervals. Data collected for fire treatment was at a rate of 10 data/sec. The fire test set up is as shown in Figure 26.

Figure 26: Furnace test setup

Initially, the trial sample was exposed to fire for one hour, and to have better understanding of temperature attained by the beam, a thermocouple was set up at the top surface of the beam. The test was run, and beam's surface temperature was recorded for an hour. It was noticed that the maximum temperature attained within the furnace was 1652°F (900°C) while the maximum temperature at the top surface of the beam was only 1121°F (605°C). Based on the flexural results from the trial sample after fire exposure of one hour, the decision was made to fire treat final samples for only 30 minutes.

The surface of final samples was cleaned before exposing them to the fire. Three thermocouples read and record the temperature attained by these samples. One among them was embedded at the midspan and midsection of the beam and the other two were attached to the top and bottom surface, respectively. Along with the beams, two cylinders were also exposed to fire, as can be seen in Figure 27, where each cylinder had one thermocouple attached to its bottom surface. For fire exposure of 30 minutes, the maximum temperature attained in

the furnace was approximately 1337°F (725°C). Table 16 shows the fire test matrix followed in this research.

Table 16: Fire test matrix for specimens

Sample No.	% of Cement Replacement	Hybrid fibers	Fire Exposed	No. of specimens		Remarks
				Beams	Cylinders	
1	0	No	No	1	2	Control
2	0	No	Yes	2	4	Control
3	20	No	No	1	2	
4	20	No	Yes	2	4	
5	0	Yes	No	1	2	
6	0	Yes	Yes	2	4	
7	20	Yes	No	1	2	
8	20	Yes	Yes	2	4	

a.

b.

Figure 27: Fire test setup: a) Specimens in the furnace; b) Specimens after fire exposure

4.2 Compressive Strength Test

The compressive strength test was performed as per the ASTM C39 (2018) standards. Cylinders with dimensions of 4 in. (0.10 m) in diameter and 8 in. (0.20 m) in height were used as test samples. Three cylinders from each mix were tested for compression strength. One cylinder was tested at room temperature, and the remaining two were tested after 30 minutes of fire exposure to report the residual compressive strength. Due to scheduling conflicts, the samples were tested at 60 days instead of 28 days. Before performing the test, the cylinders were capped at the bottom and top surface to obtain a flat surface area for loading using sulfur as per the ASTM C617 (2015) standards, as shown in Figure 28.

Figure 28: Capping of cylinders

After capping, the cylinders were set up and levelled under the 400-kip universal testing machine available at the CELB. In order to accurately record the loading of the specimen, a loading cell was set up under the cylinders. The test set up can be seen in the Figure 29. Once the test setup was complete, the testing was performed, and the load was applied at a rate of approximately 400 lb. /sec. following the ASTM C39 (2018) standards. The data collected for compressive strength was at a rate of 60 data/sec. The compressive strength was reported at room temperature and after fire exposure.

Figure 29: Compressive strength test setup

4.3 Split Tensile Strength Test

The Split Tensile Strength Test was performed following the ASTM C496 (2004) standards. A similar testing pattern was followed where a total of three cylinders were tested for split tensile strength, one at room temperature and the remaining two after 30 minutes of fire exposure. The tests were also performed at 60 days instead of 28 days due to the non-availability of the testing machine. Following the guidelines of ASTM C496 (2004), the cylinders were set up under the universal testing machine using the setup equipment. After placing the cylinder on the top of the setup equipment, a plate was placed on the top curvature of the cylinder to maintain uniform loading on the specimen during testing. The setup can be seen in Figure 30. The test was performed under a constant loading rate of 200 psi/min (42 lb. /sec.), as suggested by the ASTM standard. The data collection was at a rate of 60 data/sec. The split tensile was also reported at room temperature and after 30 minutes of fire exposure.

Figure 30: Split Tensile Strength test setup

4.4 Flexural Strength Test

The final testing setup was the flexural strength test and was performed as per the ASTM C78 specifications (2018). A three-point loading setup was used to perform the flexural test. Universal testing machine used in previous setups was also used to perform the flexural test. The setup was executed using a steel beam at the base of the testing machine which elevated the entire setup. Figure 31 shows a sketch of flexural test setup.

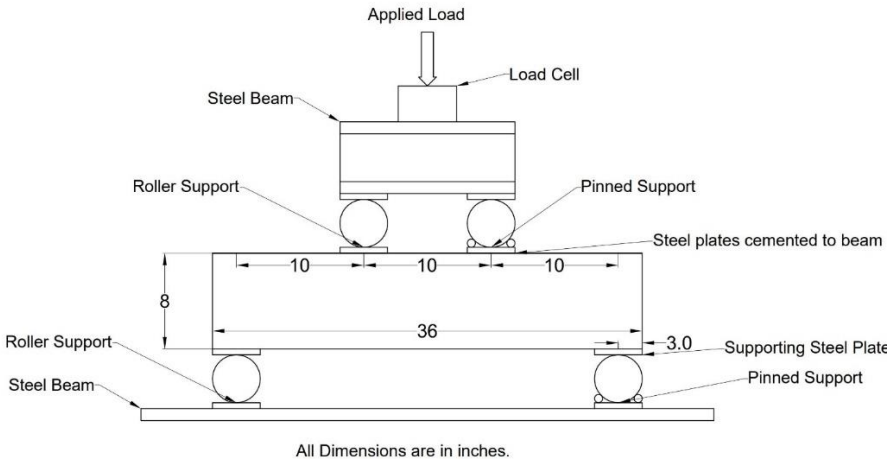

Figure 31: Flexural strength test setup sketch

As seen above, the steel beam at the bottom of the setup was centered and levelled with the universal testing machine. The steel beam was then marked for the supports to be placed. On either ends of the steel beam, a roller and a pinned support was set with 30 in. center to center distance. The beam was placed on these supports and was levelled at this stage. On top surface of this beam, two similar support setups were established and fixed to the beam using rapid setting mortar. Another steel beam was placed on these fixed supports that served as a supporting medium for the load cell that also provided even application of load from the machine. On top of the steel beam, a load cell was placed to accurately record and monitor the load applied on the beam by the testing machine. At every stage of the setup each individual element was accurately leveled. The data collection rate for flexural strength was 60 data/sec. The final flexure test setup with actual sample can be seen in Figure 32.

Figure 32: Flexural test setup with beam

To accurately monitor and record the data, such as tension and compression strains, the mid span deflection, and loading rate of the beam, numerous devices were used in the test setup. To

measure deflection, two linear variable displacement transducers (LVDT**)** were set up on either side of the beam and were attached to an angle as the bottom support. A rigid aluminum bar was cemented to the top surface of the beam at midspan section and projected on either side. The aluminum bar was firmly fixed without any movement to ensure that the obtained deflection data was accurate. The measuring ends of the LVDT's were then allowed to touch the bottom of the aluminum bar to record any displacement that occurred in the beam during testing.

Two strain gauges were additionally attached to the beam surface; one strain gauge was attached at the bottom midsection of the beam to measure tension strains and the other at the side top midsection of the beam to measure compression strains. Before attaching the strain gauges, the beam surface was smoothened using sandpaper and then cleaned using acetone. The data collection rate for strains was 10 data/sec. The two strain gauges are shown in Figure 33.

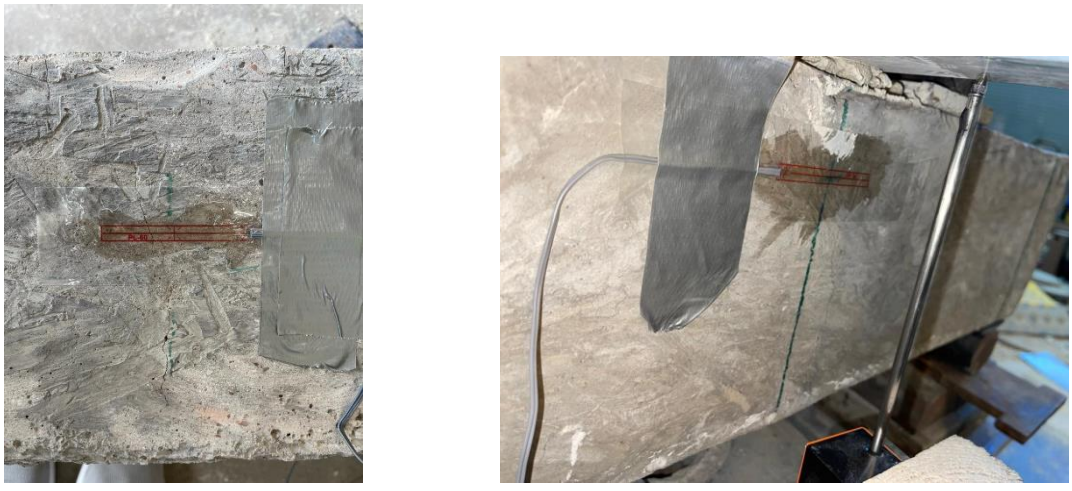

a. b.

Figure 33: Strain gauge**:** a) Tension Stain gauge; b) Compression strain gauge

Finally, to accurately monitor the load applied by the testing machine on the sample, a load cell (orange circular cell) was installed at the top of the setup. The testing machine was directly

in contact with the top surface of the load cell which helped in accurately recording the data pertaining to the loading of the specimen.

All the aforementioned measuring devices were then connected to a data collector, and once the test setup was complete, these measuring devices were turned on and calibrated directly before starting the test. Load was then applied at a constant rate of 36 lb. /sec as determined using the ASTM C78 (2018). The data was collected at a rate of 100 data/sec. During the testing, all the measuring devices were constantly monitored to ensure proper functioning, and upon completion of the test, all the data was recorded and saved. The measuring devices can be seen in the Figure 34.

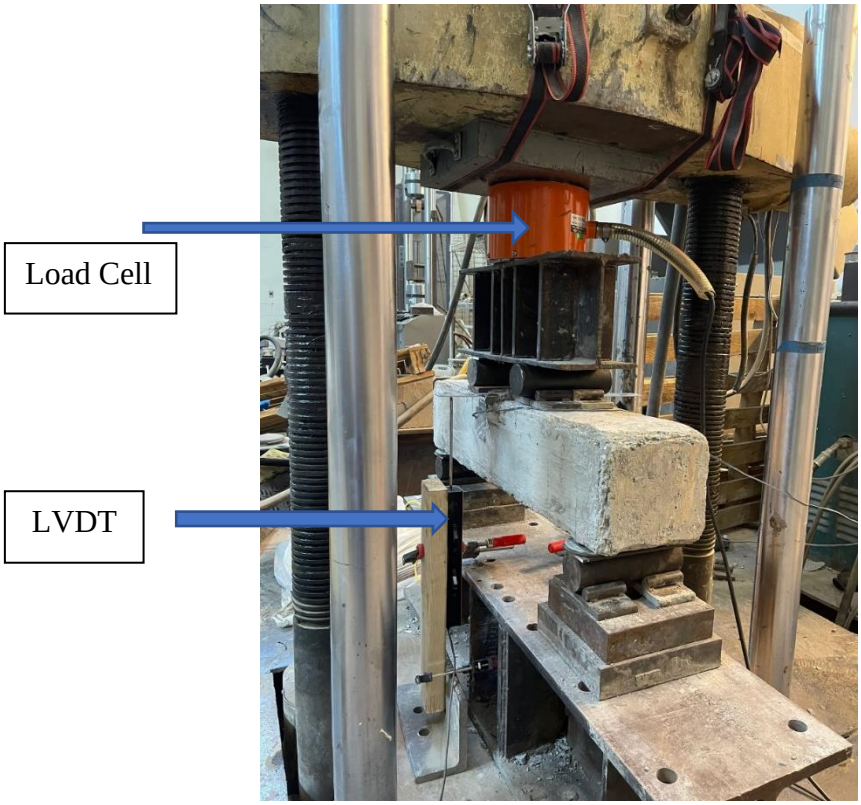

Figure 34: Test set up with measuring devices

Chapter 5

Results and Discussion

5.1 Slump Flow Test

Once the fresh concrete was produced, it was straightaway tested for slump flow as per ASTM C1611/C 1611M (2005) specifications as shown in Figure 35. The slump test mold was dampened and placed on a flat surface with the larger opening of the mold facing downwards. It was held firmly and filled with the fresh concrete in one lift and was slightly overfilled. The excess concrete was stricken off with a trowel and levelled to the top of the mold. Then the mold was lifted, and the concrete was allowed to flow onto the flat surface. Once the concrete stopped flowing, the largest diameter of concrete spread was initially measured and then another diameter, perpendicular to the initial reading, was taken. The final slump flow diameter was reported as the average of the two perpendicular diameters.

a.

b.

c.

d.

e.

Figure 35: Slump test: a) Filling of slump cone; b) Concrete levelled to top surface of slump cone; c) R-SCC; d) F-SCC; e) FG-SCC

As seen from Table 17, for a constant w/c ratio of 0.40, the mixture with 20% VCAS glass pozzolan as cement replacement; G-SCC had the maximum flow, the presence of glass pozzolan improved the workability of the mixture when compared to the R-SCC. Similar findings were observed by Ghafoori et al. (2016), where replacement of cement by natural pozzolans reported better workability of the mixture with increasing replacement percentage. On the other hand, the minimum flow was obtained for F-SCC, indicating the negative effect of fibers on workability of the mixture. The same was observed by Ding et al. (2012), where the introduction of hybrid fibers in SCC mix decreased the workability of the mixture. Further comparison could be established for reduction in workability between F-SCC and FG-SCC; reportedly the reduction for R-SCC was much higher than that of SCC with glass pozzolan (G-

SCC) when hybrid fibers are introduced in the mixture. The regular SCC had a decrease of 13% in its workability, whereas G-SCC had a reduction of only 4% with addition of hybrid fibers to the mix., whereas G-SCC had a reduction of only 4% with addition of hybrid fibers to the mix.

Table 17: Slump flow obtained for each batch of concrete mix

Mix designation	**Batch**	**Largest Diameter (D_1) (in.)**	**Diameter perpendicular to D_1 (D_2) (in.)**	**Average Diameter D ((D_1 + D_2)/2) (in.)**	**Average for the mix (in.)**	**Comments**
R-SCC	1	23	23	23		Control
	2	24	22	23	**23**	
G-SCC	1	25	25	25		
	2	23	23	23	**24**	
F-SCC	1	20	20	20		
	2	19	21	20	**20**	
FG-SCC	1	24	22	23		
	2	23	23	23	**23**	

5.2 Trial Sample Results

5.2.1 Compressive Strength

The compressive strength for trial FG-SCC sample was calculated as the average of two cylinders tested as per ASTM C39 (2018) standards and was reported as 5.77 ksi.

5.2.2 Fire Treatment

The ASTM E119 (2019) time versus temperature curve's breakdown for one hour is as shown in Figure 36. Figure 37 presents the temperature attained in the trial beam during

different stages of fire testing. For the first 30 minutes, the temperature gradually increased and was below the target temperature. At this stage, a lot of steam was observed from the furnace because of pore water pressure release, due to melting of PP fibers. This steam, however, is believed to have hindered the temperature recording of the thermocouple as it encountered the thermocouple's sensor. A closer look at the temperature recordings showed that the maximum temperature attained by the beam was 1120°F (604°C), approximately 27 minutes into the test. After this point, the temperature decreased throughout the testing time due to the hindrance in measurement caused by water and steam vapors.

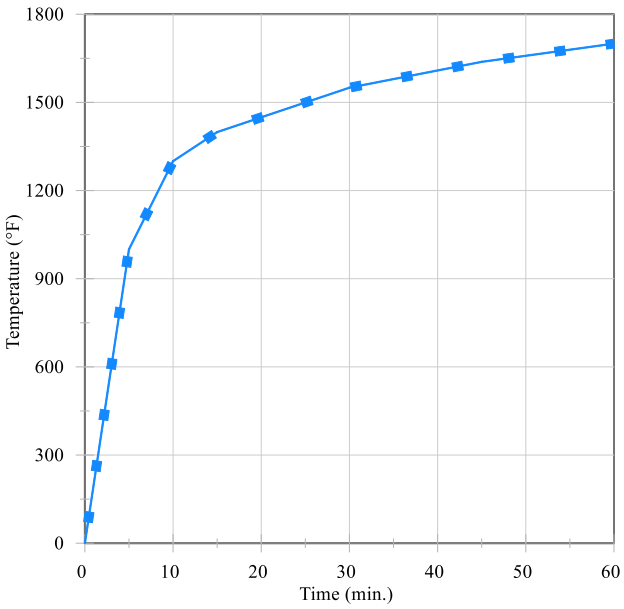

Figure 36: ASTM E119 time vs temperature curve

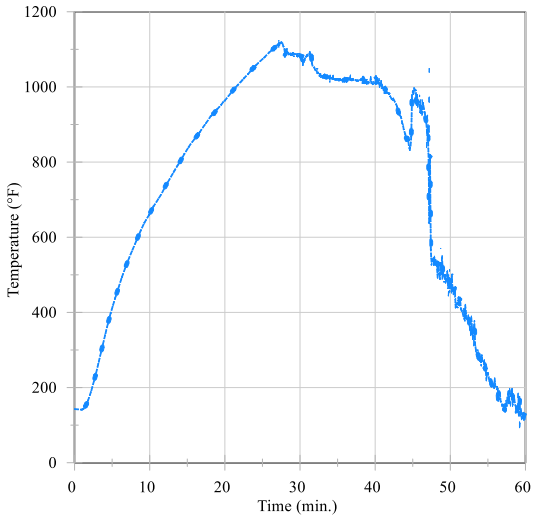

Figure 37: Time vs temperature curve for trial FG-SCC beam

5.2.3 Flexural Strength

The load versus displacement curve for the trial beam is shown in Figure 38. One hour into fire exposure made the trial FG-SCC beam so weak that it failed immediately once the machine started applying load on the specimen. The flexure strength of the beam was found to be as low as 161 lb. (0.72 kN). Since the reported flexural strength of the specimen was very low after one hour fire exposure, hence the fire exposure time was reduced to 30 minutes to obtain better flexural results for final samples to establish clear comparisons and better conclusions.

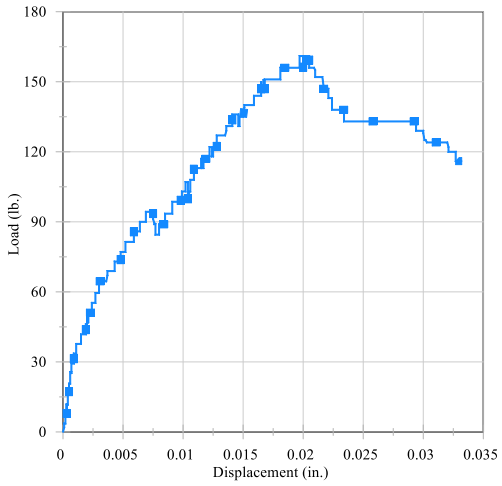

Figure 38: Load vs displacement results for trial FG-SCC beam

5.3 Fire Exposure of Final Samples

5.3.1 Beams

A total of seven beams from four different mixes were fire tested as per the ASTM E119 (2019) curve. The average temperature attained by these mixes are discussed in this section. The temperature of the furnace was set to reach 1550°F (843°C) at 30 minutes of fire exposure; however, as seen from Figure 39, these beams did not attain the said temperature and reported various temperatures at different surfaces throughout the specimen. For R-SCC, the average maximum temperature at the top surface of the beam was 1181°F (638°C), whereas for the mid-section and bottom surface it was 160°F (71°C) and 602°F (317°C), respectively. This variation of temperature measurement at different surfaces is explained using the heat flow in

the furnace. The heating coils in the furnace are located at the top surface and the heat flows from the top of the furnace to its bottom. As a result, the top half of the furnace reports higher and more accurate temperature data when compared to other locations. The average maximum temperature at the top surface of the beam for G-SCC was 1087°F (586°C); for mid and bottom section, the reported temperatures were 235°F (113°C) and 573°F (301°C), respectively. For F-SCC the average maximum temperature was as 1176°F (636°C), 185°F (85°C), and 531°F (277°C) for top, mid, and bottom surfaces, respectively. Whereas FG-SCC noted average maximum temperature was in the range of 1097°F (592°C), 210°F (99°C), and 331°F (166°C), respectively. These temperature curves are as shown in Figure 39.

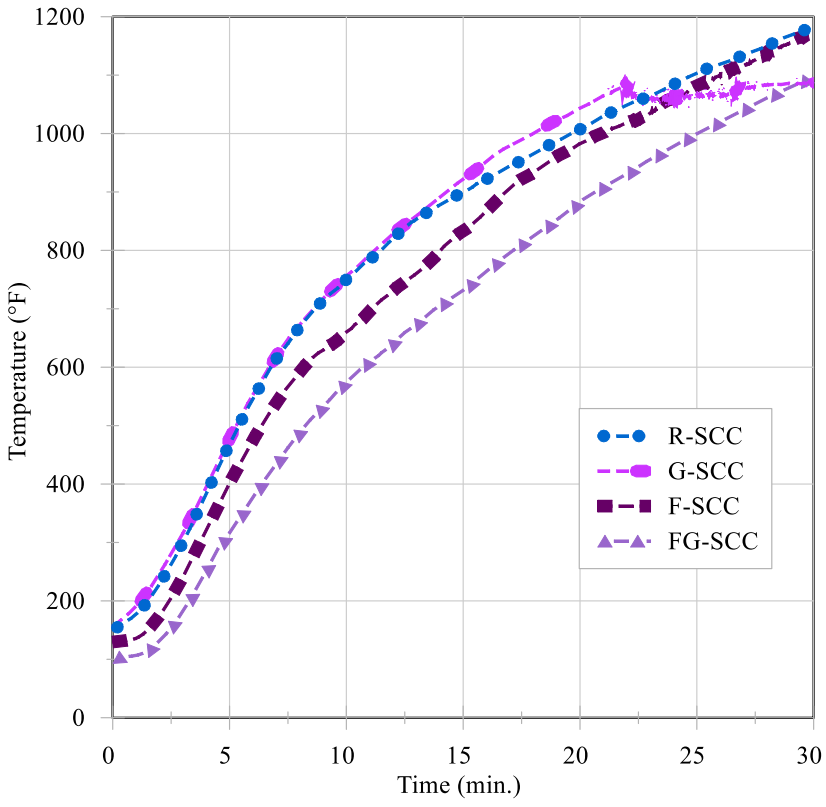

a.

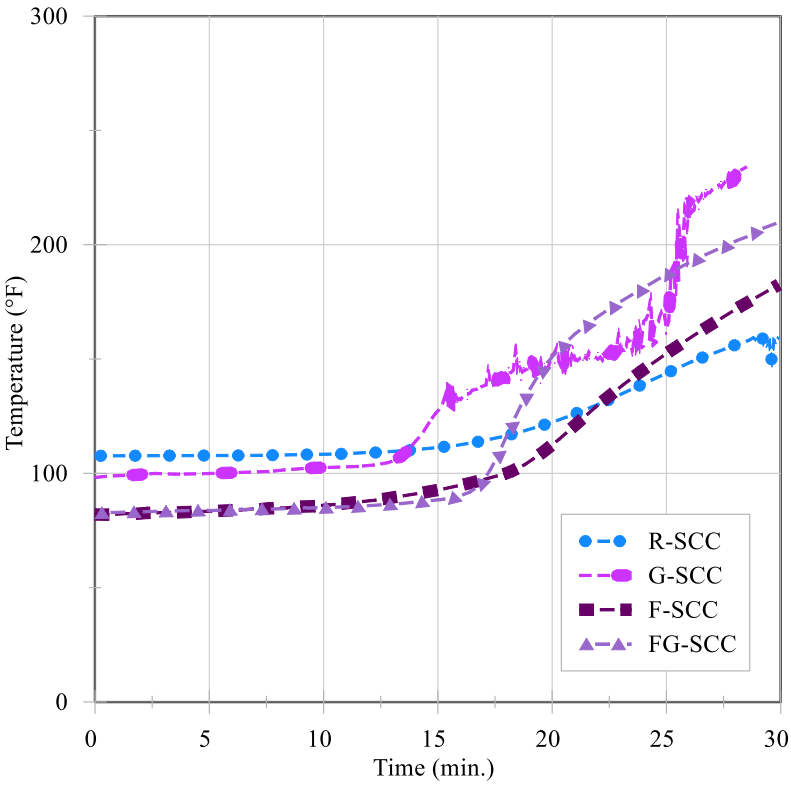

b.

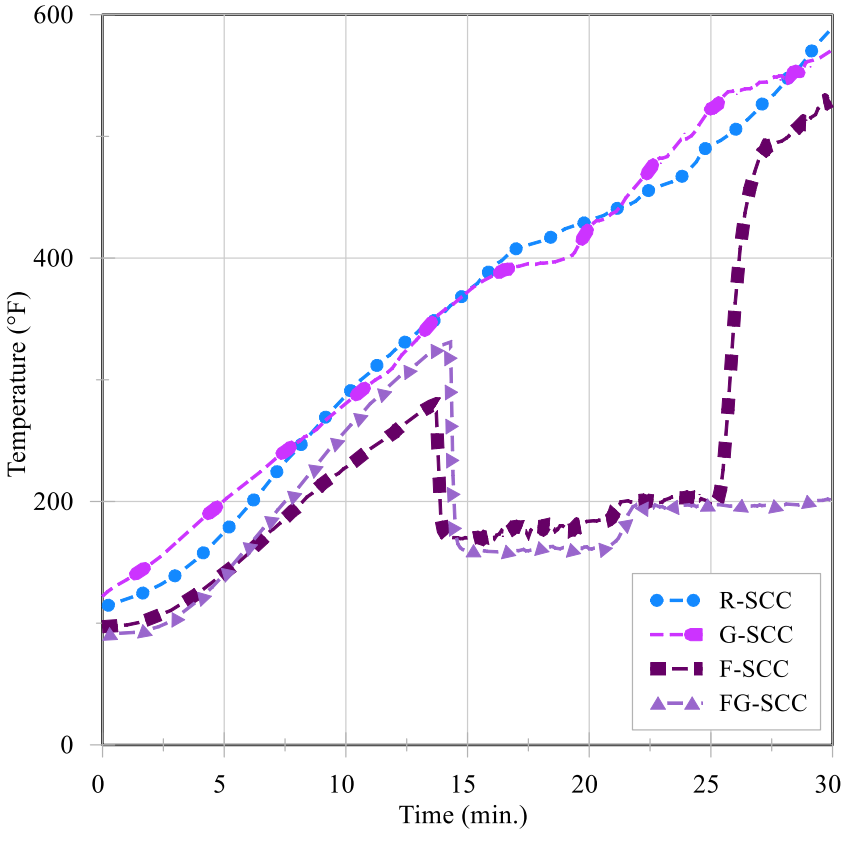

c.

Figure 39: Temperature vs time curve for all mixes: a) Top surface; b) Mid-section; c) Bottom surface

On comparing the temperatures of all the four mixes at top surface, R-SCC reported the highest temperature gain of 1181°F (638°C), whereas the least reported temperature was 1087°F (586°C) for G-SCC. The maximum temperature for G-SCC had reduction in its temperature data caused by water evaporation and can be seen in Figure 39: a. Up until this reduction, G-SCC showed higher temperature than R-SCC. For the mixes (F-SCC and FG-SCC), the intermediate temperatures were 1176°F (636°C) and 1097°F (592°C), respectively. Within the SCC and G-SCC variants, not much difference in temperature was reported and the difference observed was only 5°F (0.78°C) and 10°F (1.56°C), respectively. Whereas the mix with hybrid fibers reported least temperature for SCC, while the exact opposite was observed for G-SCC, the mix with hybrid fibers reporting the maximum temperature.

In terms of the bottom surface temperature, again R-SCC reported the maximum, 602°F (317°C). The second highest temperature observed was for G-SCC, 573°F (301°C). The mixes containing hybrid fibers had lesser temperature gain for bottom surface temperature: reportedly, 531°F (277°C) for F-SCC and 331°F (166°C) for FG-SCC. Close observation of the bottom surface temperature curve for these two mixes showed that a certain kind of disturbance is recorded in temperature measurement, resulting in lower final temperature results. While fire exposing beams containing hybrid fibers, a lot of steam vapors and condensed water was seen. This water dripped from the bottom of the furnace. This is believed to have occurred due to the melting of PP fibers within the concrete mixture. This has been previously observed by Yan et al. (2012). This observed condensed water hindered the temperature measurement when it met the thermocouple's sensor. Hence, these mixes reported lesser temperature gain for the bottom surface as seen in Figure 39: c.

The glass pozzolan variants of SCC (G-SCC and FG-SCC) reported the highest temperatures at the core (mid) section of the beam and were 235°F (113°C), and 210°F (99°C), respectively. On the other hand, SCC variants reported much lesser temperatures: 160°F (71°C)

for R-SCC and 185°F (85°C) for F-SCC. Glass pozzolan appeared to act as a thermal conductor at the core of the beams for G-SCC mix. However, at the other two surfaces the temperatures were similar for G-SCC and R-SCC with R-SCC reporting slightly higher values. The thermal conducting behavior of glass pozzolan at the core of the beam contradicted previous findings of Nasry et al. (2021); the mix with glass pozzolan showed reduced thermal conductivity than the control SCC**.** The mid-section temperature curves can be seen in Figure 39: b.

Distortions were observed in temperature curves for R-SCC and G-SCC; however, these distortions were much less when compared to the ones observed in hybrid fiber mixes at the bottom surface. Water and steam vapors were also observed for mixes without hybrid fibers; however, they were much less than the ones observed previously. Self-consolidating concrete tends to have higher moisture content than regular concrete; irrespective of hybrid fibers presence, water evaporation from the mix is observed on fire exposure. The evaporation was much higher for the mixes containing hybrid fibers because both water evaporation and melting of PP fibers occurred simultaneously. Hence, higher disturbances are seen in temperature curves for SCC with hybrid fibers.

5.3.2 Cylinders

Similarly, the cylindrical specimens from the four different mixes were fire exposed. Temperature gains were recorded for these specimens. A total of 14 cylinders were fire exposed, four each from both R-SCC and F-SCC, and three each from G-SCC and FG-SCC, respectively. The temperature curves for these mixes are as shown in Figure 40. From these curves, the maximum temperature gain for each mix was found by taking the average of all the cylinders. For R-SCC, the average maximum temperature was found to be 371°F (188°C), whereas for G-SCC it was 439°F (226°C). The mixes containing hybrid fibers reported an average maximum temperature of 307°F (153°C) for F-SCC and 323°F (162°C) for FG-SCC.

The temperature data for two of the F-SCC cylinders was lost due to a software malfunction; hence, the average obtained is based on just two specimens. As it can be seen, the maximum temperature was observed for G-SCC and the least for F-SCC. Both the mixes containing fibers reported lesser temperature gains. As previously explained, disturbances were also observed for cylindrical specimens.

When comparing two different types of specimens (beams and cylinders), beams reported much higher temperature than cylindrical specimens. The beams in the furnace were exposed to fire on all four sides and all six faces. In comparison, cylinders experienced fire exposure from top, left, and right faces only. Beams having higher surface area--8.89 ft^2 (0.826 m) -- reported higher temperature gains. On the other hand, lesser temperature gains were observed for cylinders as they had lesser surface area of 0.87 ft^2 (0.080 m^2). These specimens were cast and cured during the peak summer and hence tend to have higher internal temperatures. This can be seen in the temperature curves, where almost all curves begin around 100°F (38°C).

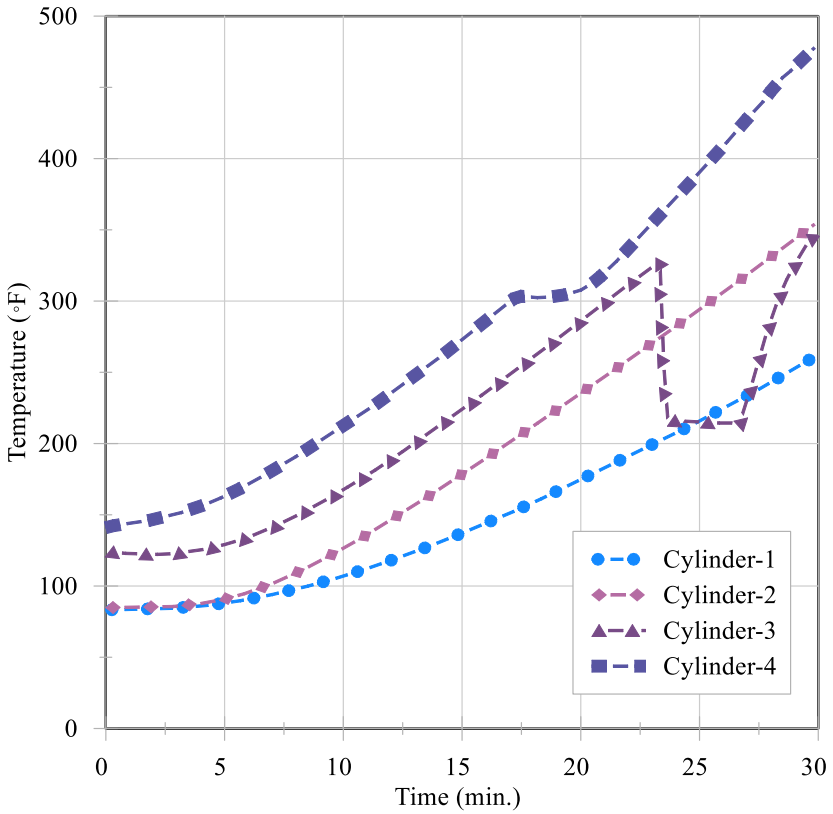

a.

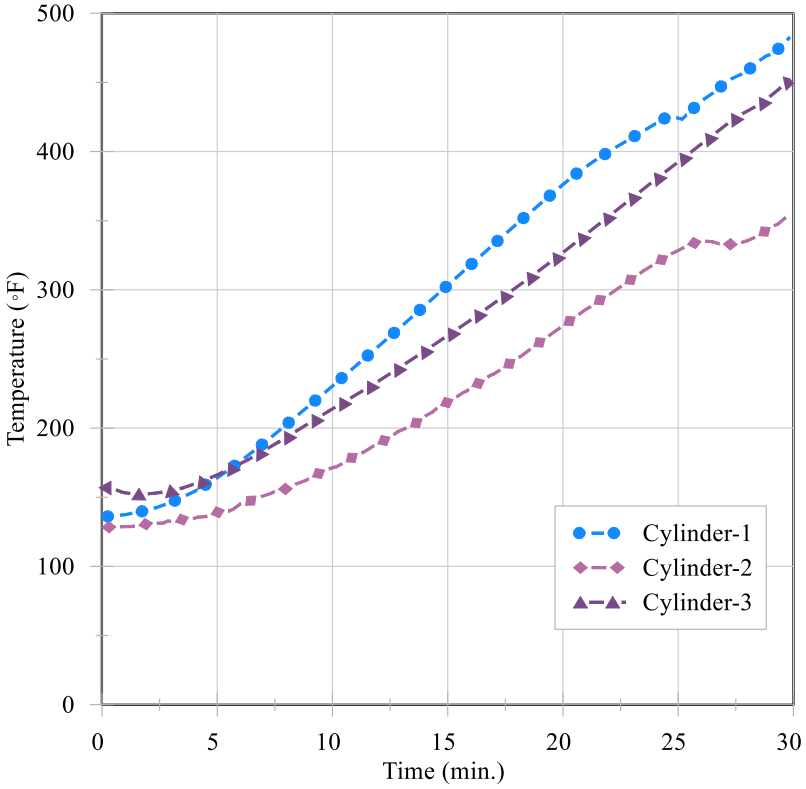
500
400
300
200
100
0
Temperature (°F)
0
5
10
15
20
25
30
Time (min.)
Cylinder-1
Cylinder-2
Cylinder-3

b.

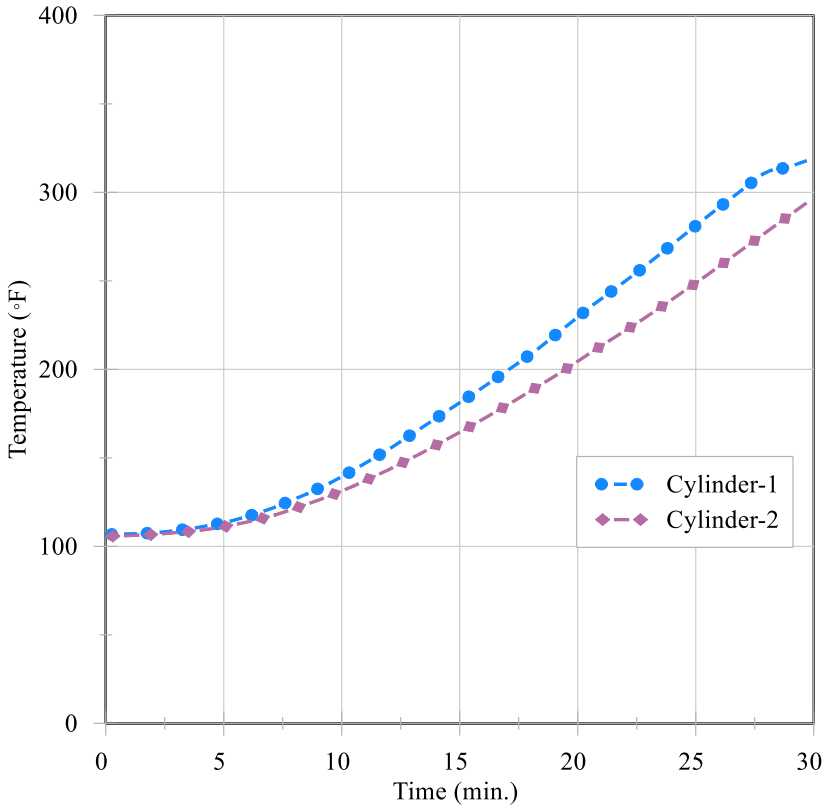
400
300
200
100
0
Temperature (°F)
0
5
10
15
20
25
30
Time (min.)
Cylinder-1
Cylinder-2

c.

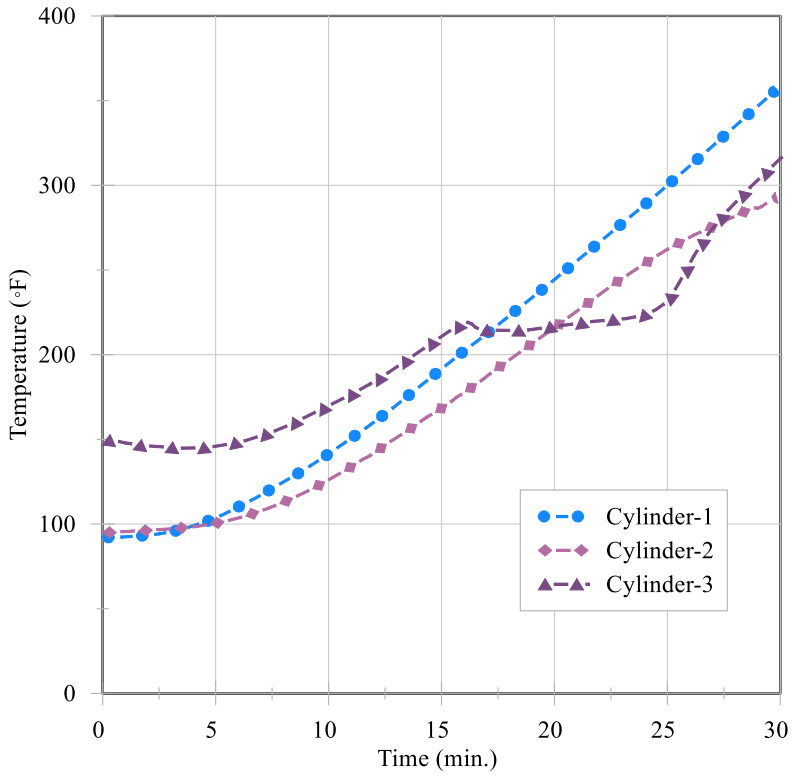

d.

Figure 40: Temperature vs time curve for cylinders: a) R-SCC; b) G-SCC; c) F-SCC; d) FG-SCC

Once the fire test was completed, beams were set aside for gradual cooling. Steel plates were used as bases to place these heat-treated beams and then the beams were allowed to gradually cool at room temperature for 24 hours. Due to fire exposure, no critical damage was observed on these beams; however, the formation of small cracks throughout the beams surface was evident. Due to the fire test, the change in temperature developed internal thermal stresses in the concrete matrix, resulting in small cracks. After the gradual cooling period, these cracks expanded and were clearly visible as they propagated throughout the beam. Majority of these beams failed along these developed cracks during the flexural strength test, resulting in more prominent structural cracks. Some of the beams also had their edges slightly damaged due to the fire exposure. Cracks were additionally seen on cylinders after fire exposure. Figure 41 shows cylinders after fire exposure that were set aside to cool gradually. Figure 42 shows cracks developed on these cylinders after exposure to elevated temperature. Figure 43 shows beams after fire exposure with visible cracks on them.

a. b.

Figure 41: Cylinders after fire exposure: a) Top view; b) Side view

a. b.

c. d.

Figure 42: Cracks developed on cylinders post fire exposure: a) R-SCC; b) G-SCC; c) F-SCC; d) FG-SCC

a.

b.

c.

d.

Figure 43: Beams showing minor cracks after fire exposure: a) R-SCC; b) G-SCC; c) F-SCC; d) FG-SCC

5.4 Compressive Strength

The ASTM C 39 (2018) requires the reported compressive strength to be the average of at least three cylinders. In order to limit the number of specimens, the compressive strength reported at room temperature is based on single cylinder test, and the strength reported post fire is the average of two cylinders. In total, four cylinders (one from each mix design) were tested at room temperature, and eight cylinders (two from each mix design) were tested at elevated temperatures. Figure 44 presents the compressive strength results at room temperature. As seen from the figure, R-SCC reported the highest compressive strength at room temperature, 5.18 ksi (35.71 MPa). The second highest compressive strength was found for F-SCC which was equal to 4.57 ksi (31.50 MPa). Least compressive strength was reported by SCC mixes containing glass pozzolan, 4.076 ksi (28.10 MPa) for FG-SCC, and 3.40 ksi (23.44 MPa) for F-SCC.

These results highlighted the negative effects of glass pozzolan on the compressive strength. Reduction of compressive strength due to glass pozzolan has been previously reported by Zidol et al. (2015) and Islam et al. (2017). Both the studies reported that glass pozzolan reduced the initial compressive strength of concrete and development in strength was only observed in long term i.e., after 90 days. No compressive strength gain was observed due to the presence of hybrid fibers. Similar findings were observed by Ding et al. (2012), where compressive strength of hybrid fiber reinforced SCC was initially lesser than the control SCC at room temperature. At the same time, slightly higher compressive strength was observed for hybrid fiber SCC with increasing percentage of steel fibers. Eventually the study reported no significant trend for increasing compressive strength.

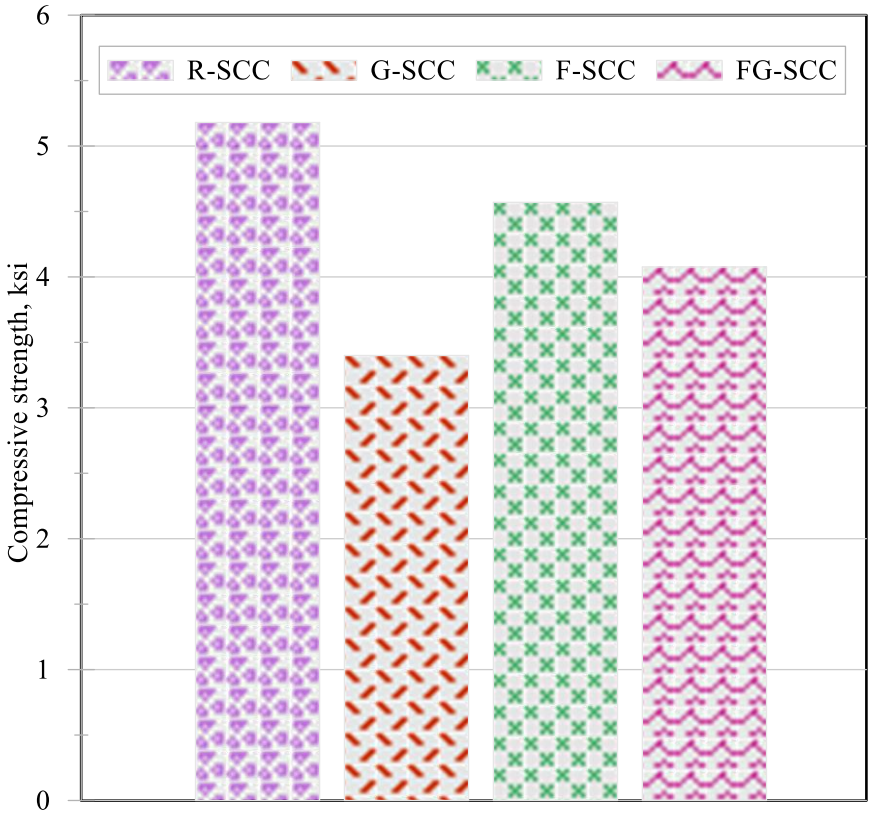

Figure 44: Compressive strength at room temperature

Figure 45 represents the compressive strength results after 30 minutes of fire exposure. Even after fire exposure, similar trends in compressive strength were observed where R-SCC reported the highest compressive strength 4.625 ksi (31.89 MPa), and G-SCC being the least at 2.78 ksi (19.16 MPa). Mixes containing hybrid fibers, F-SCC and FG-SCC reported 3.92 ksi (27 MPa), and 3.40 ksi (23.44 MPa), respectively. Percentage reduction for the four mixes, R-SCC, G-SCC, F-SCC, and FG-SCC were 11%, 18%, 14%, and 16%, respectively. Percentage reduction was least for R-SCC and maximum for G-SCC, while F-SCC and FG-SCC reported intermediate percentage reductions. The presence of steel fibers did not aid the compressive strength of the concrete at room as well as elevated temperature.

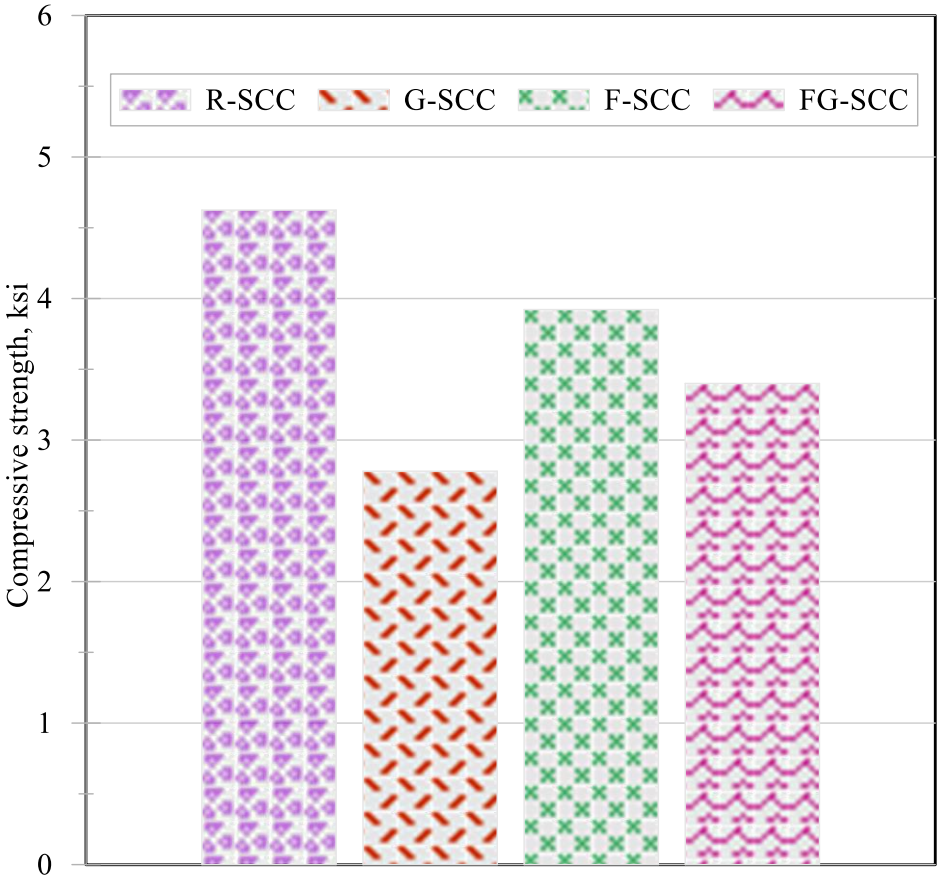

Figure 45: Compressive strength at elevated temperature

The failure patterns for cylinders at room temperature are as shown in Figure 46. Typical failure patterns that occur in cylinders, presented by ASTM C39 (2018) standards are as shown in Figure 47. The failure pattern observed for R-SCC, G-SCC, and FG-SCC was type 3, where vertical cracks were observed from both ends of the cylinder and there were no well-formed cones. While for F-SCC, the failure pattern was Type 2, where cracks generated at the top of the cylinders, travelled towards the bottom, and formed a cone at the bottom end.

a.

b.

c.

d.

Figure 46: Failure pattern for compression cylinders at room temperature: a) R-SCC; b) F-SCC; c) G-SCC; d) FG-SCC

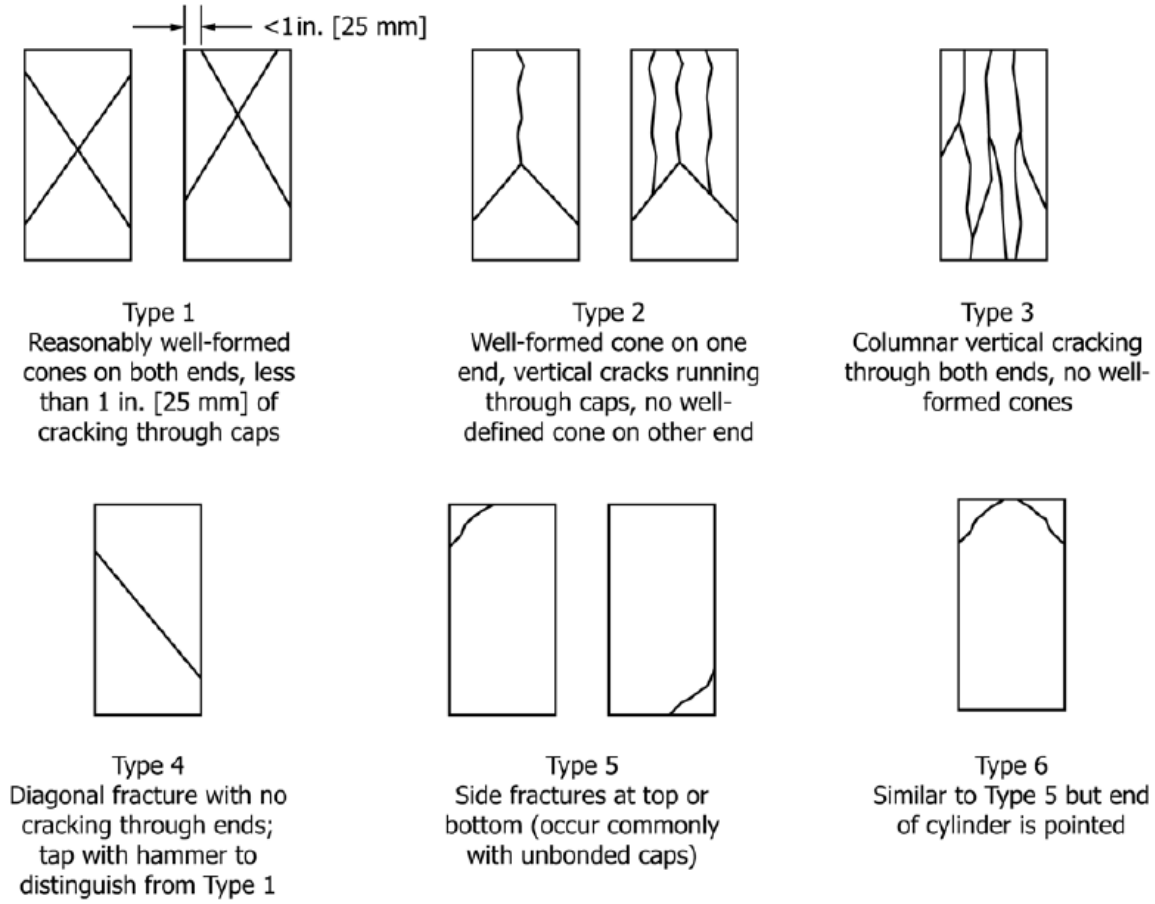

Figure 47: Typical failure modes as per ASTM C39 (2018)

After fire exposure, the failure mode for R-SCC did not change and vertical cracks were seen throughout the specimen. Whereas, for F-SCC, the failure mode changed to Type 3. Failure pattern for G-SCC and FG-SCC post fire exposure, were not clear enough and hence could not be classified as per standard failure patterns. These failure modes post fire exposure can be seen in Figure 48.

a.

b.

c.

d.

Figure 48: Failure pattern for compression cylinders at elevated temperature: a) R-SCC; b) F-SCC; c) G-SCC; d) FG-SCC

5.5 Split Tensile Strength

A similar trend was followed for split tensile as mentioned for compressive strength where a total of four cylinders (one from each mix) was tested at room temperature, and an average of two cylinders per mix was reported post 30 minutes fire exposure. The split tensile strength results as per ASTM C496 (2004) at room temperature is shown in Figure 49. As seen from the figure, the maximum split tensile strength was again observed for R-SCC, 580 psi (4 MPa). While G-SCC, F-SCC, and FG-SCC reported 501 psi (3.45 MPa), 533 psi (3.67 MPa), and 525

psi (3.62 MPa), respectively. Split tensile strength followed the same trend as the compressive strength at room temperature where least strength was observed for G-SCC, while FG-SCC reported slightly better strength. Mix containing hybrid fibers (F-SCC) reported lesser tensile strength than R-SCC, highlighting that, fibers did not show any positive effects on split tensile strength at room temperature.

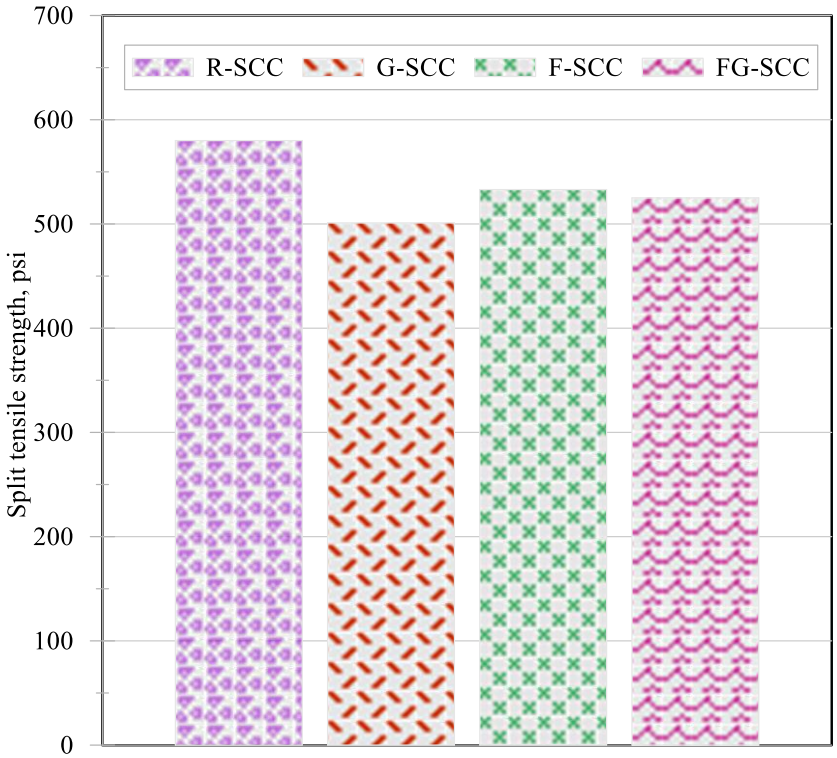

Figure 49: Split tensile strength at room temperature

Split tensile strength at elevated temperatures is shown in Figure 50. Post fire, the maximum split tensile strength, 415 psi (2.86 MPa) was observed for FG-SCC. Once again, the least strength observed was for G-SCC, 376 psi (2.6 MPa). The other two mixes, R-SCC, and F-SCC reported 385 psi (2.65 MPa), and 404 psi (2.78 MPa), respectively. SCC incorporating hybrid fibers showed lesser percentage reduction than SCC without any fibers. Percentage reduction for FG-SCC and F-SCC were 21% and 24%, respectively. While for the mixes without hybrid fibers, G-SCC and R-SCC were 24% and 34%, respectively. Regular SCC had the maximum reduction in strength after fire exposure. Presence of hybrid fibers slightly benefitted the split tensile strength post fire exposure. No previous research explaining

the split tensile strength for SCC with hybrid fibers and glass pozzolan at different temperatures was found, and thus no comparison could be established.

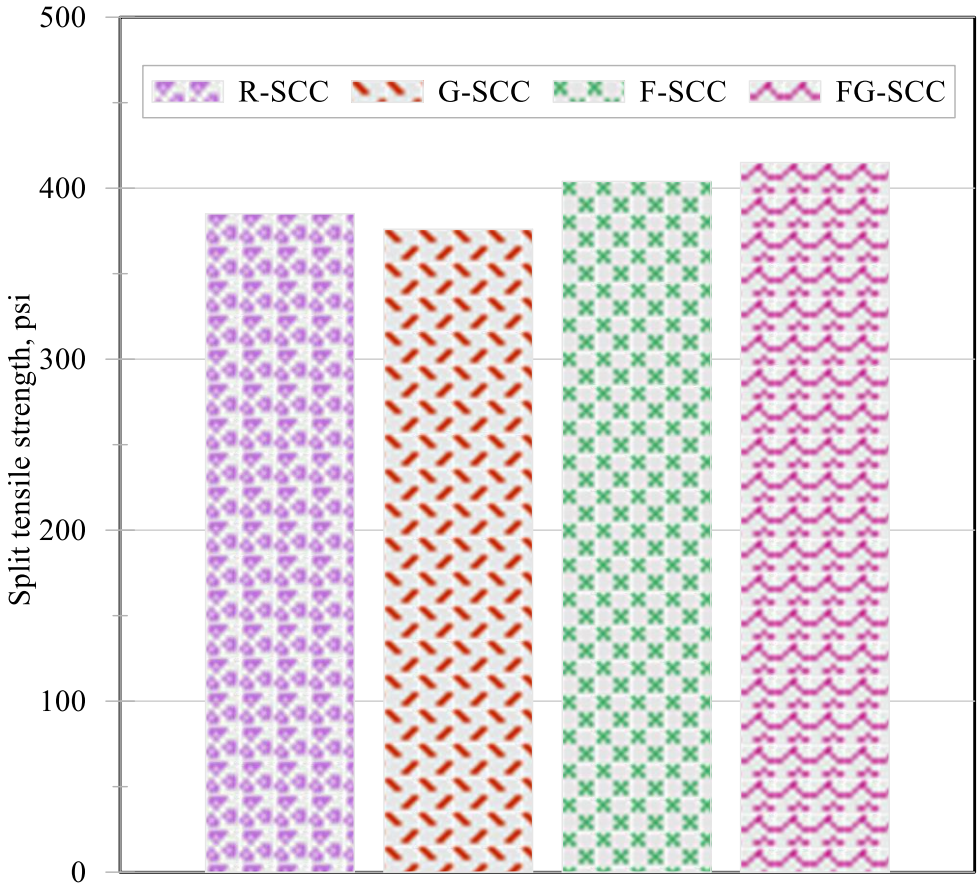

Figure 50: Split tensile strength at elevated temperature

Typical failure pattern was observed for split tensile strength where cracks formed on the face of the cylinder, ran across the face, and split the cylinder into two. The failure planes for some of the cylinders are as shown in Figure 51.

a.

b.

c. d.

Figure 51: Typical failure patterns observed for split tensile strength test: a) R-SCC; b) G-SCC; c) F-SCC; d) FG-SCC

5.6 Flexural Strength

The flexural strength of the four mixes at room temperature are as shown in Figure 52. As seen from the figure, the maximum flexural strength at room temperature was observed in R-SCC, 12.4 kip (55.16 kN). The mix with glass pozzolan and hybrid fibers, FG-SCC reported least strength of 9.40 kip (41.81 kN). Same flexural strength of 11.80 kip (52.49 kN) was observed for both F-SCC and G-SCC. The SCC with hybrid fibers (F-SCC) showed lesser strength when compared to control SCC, these results contradicted previous findings (Ding et al., 2012). These findings proved that at room temperature, presence of hybrid fibers did not aid the flexural strength. However, the difference obtained for flexural strength was not significant enough to conclude that negative effects were observed due to the hybrid fibers. On comparing the glass pozzolan variants of SCC, FG-SCC reported least strength at room temperature. The combination of glass pozzolan and hybrid fibers in the concrete mix affected the flexural strength significantly.

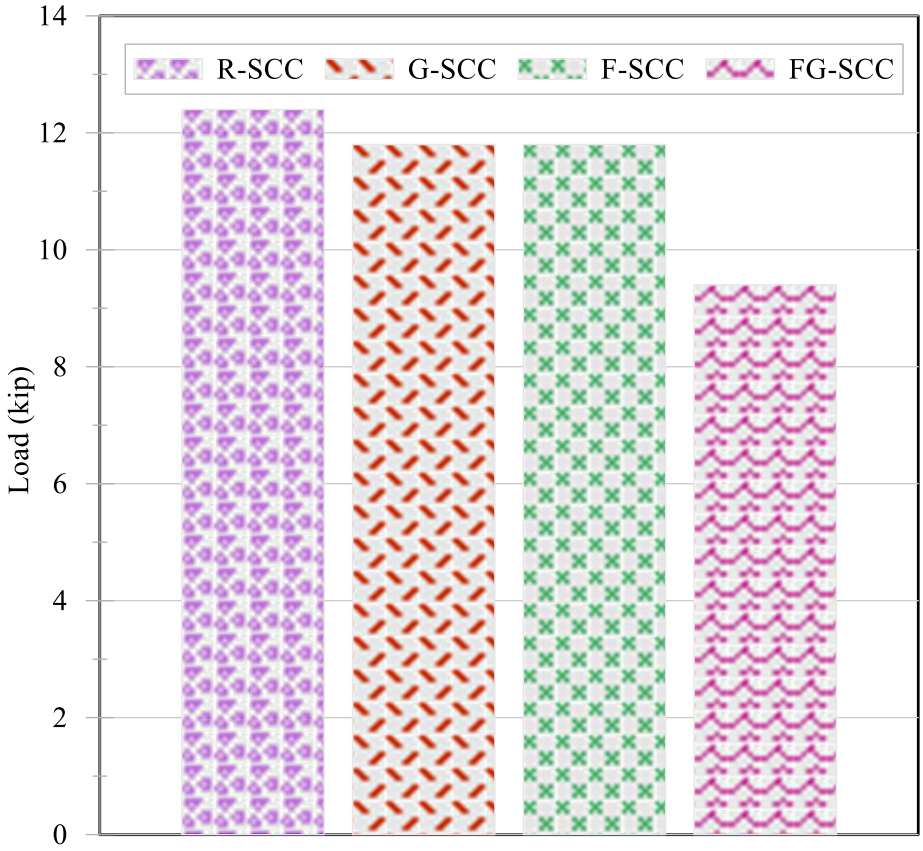

Figure 52: Flexural strength at room temperature

Figure 53 shows load versus displacement data for the fractured beams at room temperature. The maximum displacement observed was for R-SCC, 0.32 in (8.4 mm). While G-SCC failed at a lower strength and reported displacement of 0.25 in. (6.35 mm). The load vs displacement curve for F-SCC and G-SCC followed similar load paths and these beams failed at the same load, 11.80 kip (52.49 kN). The displacement for these beams observed was 0.28 in. (7.11 mm). All these beams failed had a brittle failure as can be seen in Figure 53, where a sudden drop in ultimate load is observed indicating the failure point.

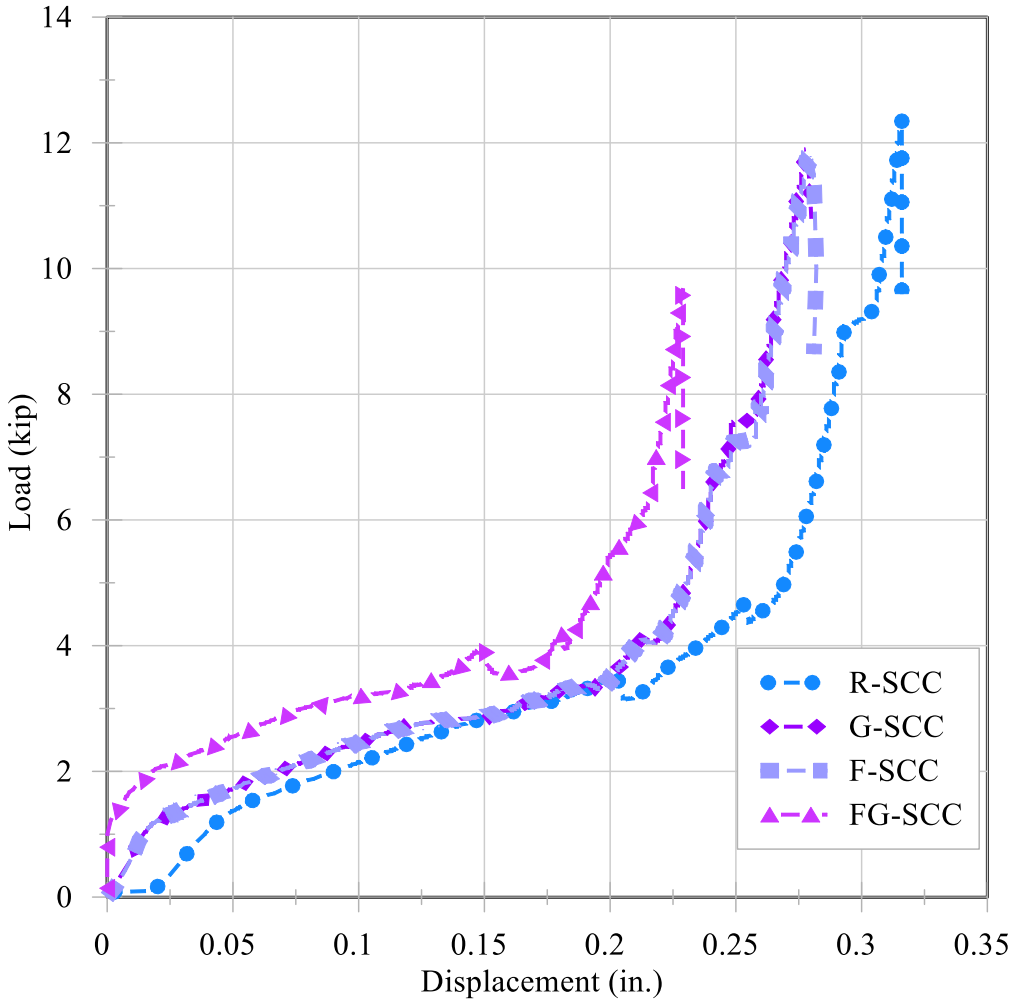

Figure 53: Load vs displacement curve at room temperature

Tensile and compressive strains data obtained at room temperature is shown in Figure 54. On comparing the tensile strains, concrete mixes with glass pozzolan reported higher tensile strains. The highest compressive strains were observed for FG-SCC. The tensile strains for R-SCC and F-SCC were comparable however, F-SCC reported higher compressive strains than R-SCC. Compressive strains for F-SCC and G-SCC were quite similar. The failure pattern for all the beams was similar at room temperature where, beams failed in brittle manner and cracked through the middle section. One such failed beam is as shown in Figure 55.

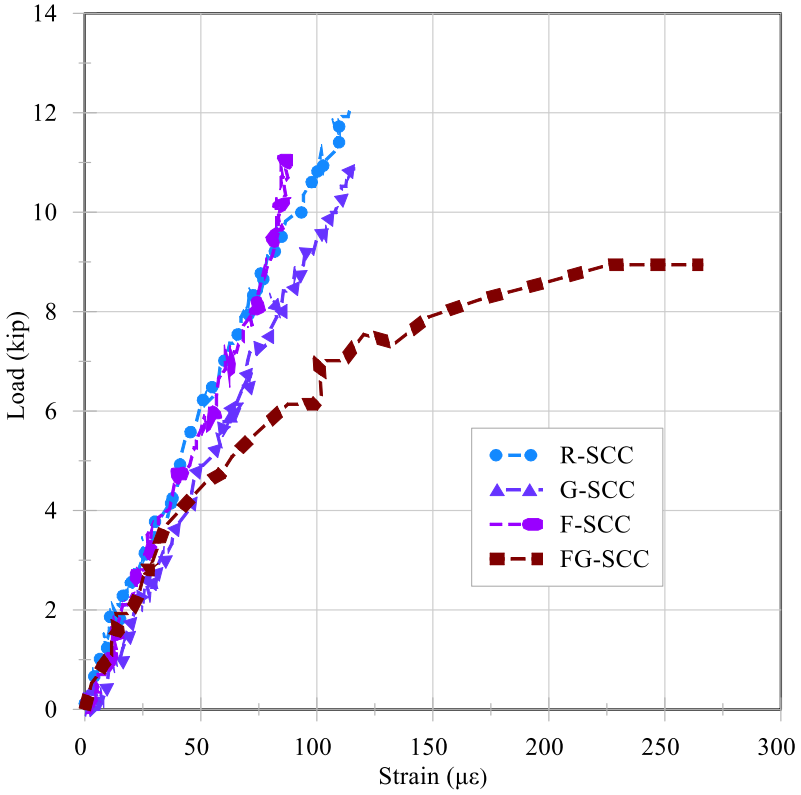

a.

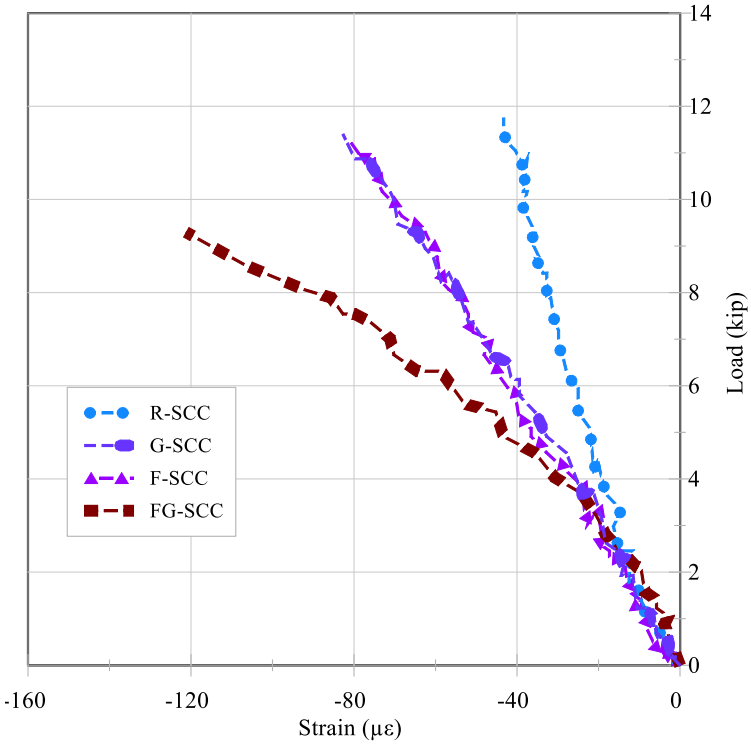

b.

Figure 54: Load vs strain curves: a) Tensile strains; b) Compressive strains

Figure 55: Beam failure pattern after flexure test

One beam each from mix G-SCC and FG-SCC was damaged and could not be tested for residual flexural strength. The beam from mix G-SCC was damaged during the test setup after fire exposure. The beam was too weak to even withstand the load of the set up and failed before the testing could begin. The beam from FG-SCC was lost due to the malfunctioning of the hydraulic machine used to transport beams during testing. Figure 56 shows the flexural strength of the different SCC mixes post fire exposure. Regular SCC (R-SCC) that reported highest strength at room temperature, had least flexural strength post fire exposure, 325 lb. (1.45 kN). The percentage reduction observed was as high as 98% as if there was zero load resistance post fire exposure. Mix containing hybrid fibers and glass pozzolan (FG-SCC) that had least flexural strength initially, reported the highest strength 916 lb. (4.07 kN) at elevated temperature. The percentage reduction was 90% for these beams and the lowest among all the samples. Second least reduction in strength was observed in SCC containing hybrid fibers, F-SCC reported a flexural strength of 699 lb. (3.11 kN) with percentage loss of 94%. Mix with glass pozzolan (G-SCC) gave a flexural strength of 479 lb. (2.13 kN) with 96% loss in its initial strength.

After fire exposure, benefits of adding hybrid fibers were clearly observed and the concrete mixes containing them, reported highest flexural strengths. All the concrete mixes showed

ductile behavior at elevated temperature, except for R-SCC, it showed a sudden failure, and the failure pattern was similar to the one observed at room temperature (Figure 55). For other mixes the failure was ductile. The specimens did not break at all, they stopped taking any further load and showed no flexural strength beyond this point. The beams failed due to development of major cracks.

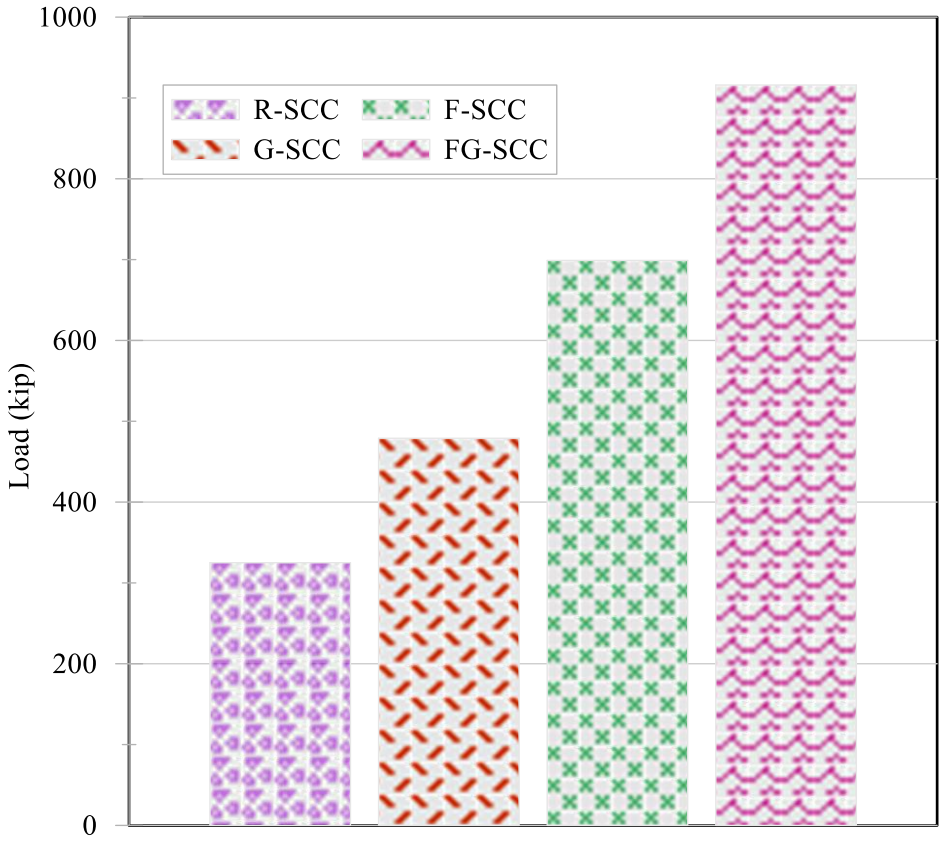

Figure 56: Flexural strength at elevated temperature

Figure 57 shows the load versus displacement curve for flexural test post fire exposure. As seen, the load versus displacement curves for mix G-SCC, F-SCC, and FG-SCC show ductile behavior. The displacement at ultimate load was higher for mixes containing hybrid fibers than the ones without them. Mix F-SCC showed a displacement of 0.05 in. (1.27 mm) at failure load. The load versus displacement curve plotted for F-SCC is obtained from a single specimen that failed at a load of 780 lb. and not as the average of the two specimens and hence the observed load is higher than the average load of 699 lb. While, FG-SCC had a displacement of

0.038 in. (0.97 mm). The displacement for R-SCC and G-SCC was much smaller comparatively and was in the range of 0.013 in. (0.33 mm).

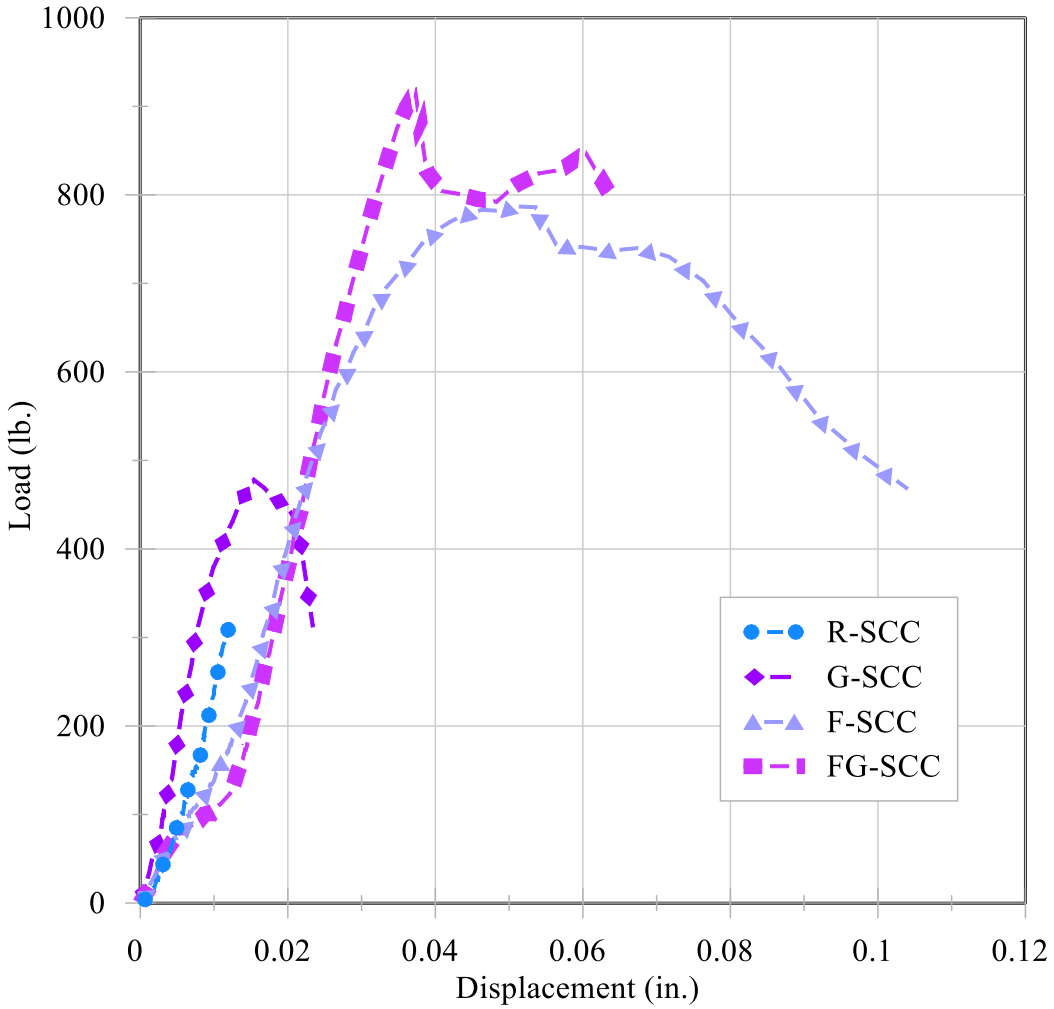

Figure 57: Load vs displacement curve at elevated temperature

Beams without hybrid fibers, R-SCC and G-SCC had an early load failure and did not report reliable strain data. However, mixes with hybrid fibers, F-SCC, and FG-SCC, did show some tensile strain data post fire exposure and can be seen in Figure 58. The SCC mix containing glass pozzolan and hybrid fibers, FG-SCC showed very high tensile strains post fire exposure highlighting the ductile behavior also SCC with hybrid fibers, F-SCC showed thrice the tensile strains observed at room temperature, once again indicating ductile behavior due to the presence of fibers post fire exposure.

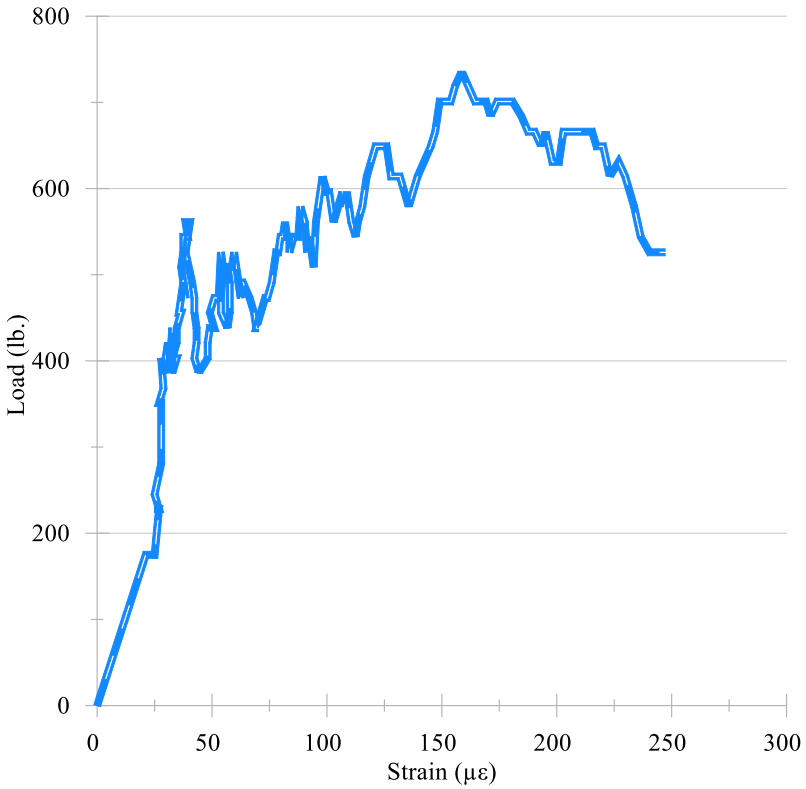

a.

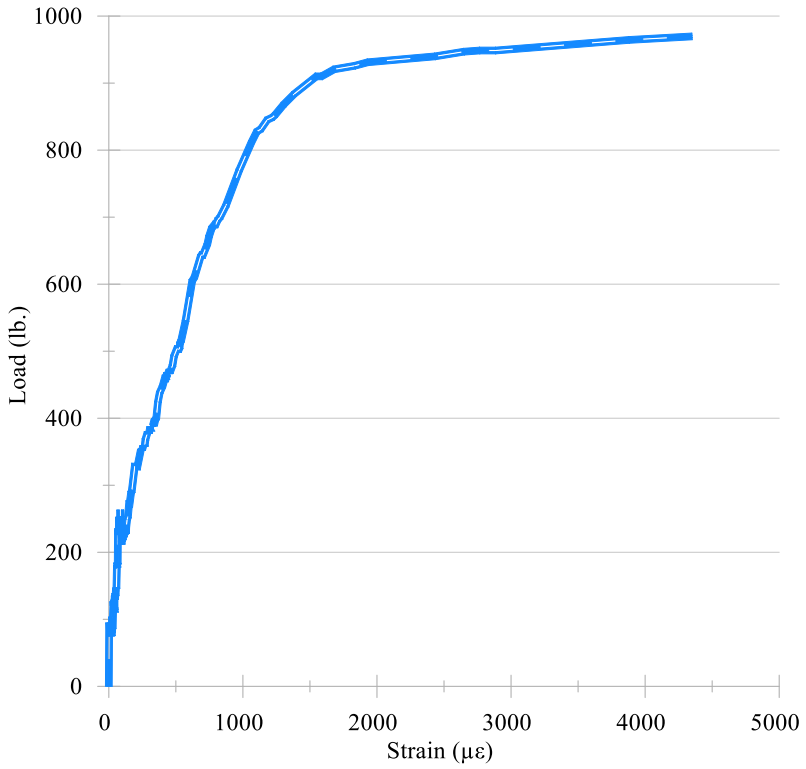

b.

Figure 58: Tensile stain curves post fire exposure: a) F-SCC; b) FG-SCC

To better understand the failure of beams after fire exposure, crack patterns of a two beams after failure were recorded and are presented below. Figure 59 and Figure 60 presents crack propagation for two such beams. The failure crack is clearly visible and can be seen running throughout the beam on different faces. These cracks were typically developed due to fire exposure, however initially they were minor cracks and after flexural tests, these cracks developed into major cracks due to loading and the beams failed along them. Similar behavior was observed in other beams where a minor crack after fire exposure turned into a major one due to flexural loading, causing failure of the beam.

a.

b.

c.

Figure 59: Crack propagation for a failed beam after fire exposure: a) Left face; b) Right face; c) Bottom face

a. b.

Figure 60: Failure crack post fire exposure: a) side face; b) bottom face

Post fire exposure, the reductions observed for flexural members were significantly higher when compared to compression members. Concrete being strong in compression resisted strength deterioration due to fire exposure significantly. Hence, post fire smaller reductions are observed for cylinders (up to 33%). As there was no steel reinforcement provided, reduction in flexural strength were much larger at elevated temperature (up to 98%). Also, flexural members experienced more heat in the furnace than cylinders as they have larger surface area exposed to fire. Therefore, higher strength reductions were observed for beams than cylinders after fire exposure.

Chapter 6

Conclusions and Recommendations

6.1 Conclusions

Four different mixes designed using combinations of cementitious material and hybrid fibers were tested for compression, tension, and flexural behavior at room and elevated temperatures. Steel and polypropylene fibers were used as hybrid fibers. In total, 12 beams and 24 cylinders were tested for the aforementioned properties as per ASTM standards. Fire exposure of these specimens were as per the ASTM E119 (2019) curve. Based on the concrete mix designs, sample preparations, test performance, and results obtained in the research, the following conclusions were made:

- The use of glass pozzolans tends to increase the workability of the SCC mix, even more so than the workability of the regular SCC. However, hybrid fibers significantly reduced the workability of the SCC mix. With glass pozzolan, the reductions were significantly lower when compared to the reductions of conventional SCC.
- The temperatures for standard SCC and SCC with glass pozzolan were similar for the top and bottom surfaces. However, at the core of the beam, glass pozzolan acted as a thermal conductor, and SCC with glass pozzolan reported a much higher temperature than the temperature of standard SCC. The temperature variations between conventional SCC and SCC made with glass pozzolan contradicted the findings of Nasry et al. (2021) where glass pozzolan behaved as an insulator and reduced the thermal conductivity of the mix. Mixes with hybrid fibers reported slightly lower temperatures comparatively.
- Hybrid fibers did not aid the compressive strength and tended to decrease the strength. The reduction was greater at elevated temperatures than at room temperature. Glass

pozzolan reduced the strength significantly and reported lower strengths at room and elevated temperatures. Similar findings were observed by Ghafoori et al. (2020). The researchers reported reductions in strength up until 90 days during the curing period and after this increase in strength was observed.

- Hybrid fibers did not show any improvement in compressive, split tensile, or flexural strength at room temperature. At elevated temperatures, hybrid fibers resisted strength deterioration, and the highest strengths, in terms of split tensile and flexural strength, were observed for mixes that contained both hybrid fibers and glass pozzolan.
- Hybrid fibers and glass pozzolan additionally tended to decrease the flexural strength at room temperature. The combination reduced flexural strength significantly and reported the least strength among all other mixes. Whereas, after fire exposure, the same combination had the highest residual flexural strength while the lowest flexural strength was observed for standard SCC.
- Hybrid fibers had a positive effects on split tensile and flexural strength post fire exposure only.
- All mixes at room temperature exhibited brittle failure. Post-fire exposure, the mixes containing hybrid fibers and/or glass pozzolan reflected a ductile behavior while the standard SCC showed brittle failure.

Hybridization is a propitious technique to reinforce concrete against fire hazards. The combination of steel and polypropylene fibers proved to be beneficial in the SCC mixture. This combination effectively tackles fire's deteriorating effects and produces better residual strength. Even at room temperature, it does not significantly affect the concrete's strength. It can reduce the possibility of loss of life caused by a collapse of structures from fire hazards in addition to providing sufficient warning signs. For the construction of structures that are highly prone to fire hazards, hybrid fibers should be considered while designing

concrete. Glass pozzolan can successively substitute cement in the concrete mixture, especially for SCC that requires high workability. Glass pozzolan has proven to be beneficial for concrete (Tapia, 2020) and even for SCC, it can provide higher strength gains after the 90-days curing period. Additionally, substituting cement with glass pozzolan can reduce CO_2 emissions from cement production and make concrete more sustainable and environment friendly. Use of glass pozzolan can, moreover, ameliorate the problem of accumulation of glass in landfills across the United States and can put a vital and abundant resource to work.

6.2 Limitations

The research also observed some of the limitations as follows:

- A trial test of an hour fire exposure of the specimens resulted in a significant damage leading to zero post-fire residual strength. Hence, the investigation was limited to half an hour exposure time to conduct the intended comparative study among the different mixes.
- ASTM E119 (2019) requires conditioning test specimens to moisture content ranging from 50 to 75% relative humidity prior to fire testing, proved to be effective for vibrated concrete. However, this requirement was not achieved in the current study due to high-water content of the SCC mix. This calls for an investigation to develop an effective conditioning method/s that is/are specifically tailored to SCC.
- The current study investigated the pre-, during and post-fire performances of 60 days old specimens. Thus, it is recommended conducting similar investigation employing accelerated aging testing protocol to evaluate long-term durability of these concrete mixes.

6.3 Recommendations for Future Work

The following recommendations are made for future research involving hybridization of self-consolidating concrete and cement replacement using glass pozzolan:

- Study the behavior of SCC for different dosage rates of hybrid fibers and recommend optimum dosing rates.
- Hybridize SCC using other macro and microfibers, quantify their advantages and disadvantages, and comment on the optimum dosage rates using these fibers.
- Study different replacement rates for cement using glass pozzolan in SCC with hybrid fibers in order to recommend the right mixing proportions for this variant of SCC to benefit strength at earlier stages.
- Study the bonding effects of hybrid fibers and steel reinforcements.
- Perform SEM and XRD analysis, characterize hybrid fiber reinforced concrete based on physical and chemical characteristics.
- Perform detailed study on crack patterns alongside their propagation after fire exposure and suggest methods to diminish these cracks.
- Study replacement of cement using other SCMs for hybrid fiber reinforced SCC.

APPENDIX

Appendix A: Mix design for the SCC mixes

Specimen volume:

- Beam – 36 in. x 8 in. x 8 in. (1yd x 0.23yd x 0.23yd)
  - Volume of one beam = 0.053 yd^3
  - Number of beams per mix = 03
  - Total volume of beams per mix = 0.16yd^3

- Cylinder – 2 in. (0.056yd) radius, 8 in. (0.23yd) height.
  - Volume of one cylinder = 0.0023 yd^3
  - Number of cylinders per mix = 06
  - Total volume of cylinders per mix = 0.014 yd^3

Total volume required per mix = 0.16 yd^3 + 0.014 yd^3 = 0.174 yd^3

Percentage assumed for extra materials = 40%

Final volume required per mix = 1.4 x 0.174 = 0.25 yd^3

Mix Design:

- Mix design assumptions based on ACI 237.7R (2007) (Table 4.1 & 4.2)
  - Percentage of coarse aggregate (CA) assumed = 32% (For Agg size > ½ in. (12mm))
  - Percentage of paste fraction assumed = 38%
  - Percentage of mortar fraction assumed = 100% - percentage of CA

    = 100% - 32%

    = 68%

- Percentage of FA = 68% - 38% = 30%
- Powder Content assumed = 650 lb./yd^3 (for slump flow 22 – 26 in. (550 - 650 mm))
- Assumed w/cm = 0.40 (range = 0.32 – 0.45)
- Fibers Dosage (recommended by Euclid Chemicals)
    1. Steel fibers = 3.5 lb./yd^3
    2. Polypropylene fibers = 1.5 lb./yd^3

Mix Design for 1 yd^3:

Powder content = 650 lb./yd^3

Water/cement ratio = 0.40

Water content = 0.40 x 650 = 260 lb./yd^3

20% Glass Pozzolan = 650 x 0.20 = 130 lb./yd^3

Cement content = 650 – 130 = 520 lb./yd^3

Volume of C.A = 32/100 x 27 = 8.64 ft^3 / yd^3

Weight of C.A = 8.64 x 100 pcf = 864 lb./yd^3

(Where, unit weight of C.A = 100 pcf)

Volume of F.A = 30/100 x 27 = 8.1 ft^3 / yd^3

Weight of F.A = 8.1 x 2.65 x 62.4 = 1340 lb./yd^3

(Where, Specific Gravity of F.A = 2.65, υ = 62.4 lb./ft^3 (Specific weight of water))

- R-SCC (regular SCC):
    - Volume = 0.25 yd^3
        1. Cement = Total volume x Powder content

           = 0.25 x 650 $lb.yd^3$

           = 162.5 lb.
        2. FA = Total volume x FA content

           = 0.25 x 1340 = 335 lb.
        3. CA = Total volume x CA content

           = 0.25 x 864 = 216 lb.
        4. Water = Total volume x water content

           = 0.25 x 260

           = 65 lb.

- F-SCC (regular SCC with hybrid fibers)
    - Volume = 0.25 yd^3
    - All quantities remain same as mix R-SCC, only addition of fibers is an extra step in this mix.
    - Fiber Content calculation.
        1. Steel Fibers = Assumed dosage x volume of the mix

           = 3.5 $lb./yd^3$ x 0.25 = 0.875 lb.
        2. Polypropylene Fibers = Assumed dosage x volume of the mix

           = 1.5 $lb./yd^3$ x 0.25 = 0.375 lb.

- G-SCC (regular SCC with 20% Glass Pozzolan (GP) as cement replacement)
    - The CA, FA, water content remains same as per the mix design of Mix A, only the Powder content changes.
    - In this mix, 20% cement is replaced by GP.
    - Glass Pozzolan required = 20% of Cement Content

$$= 20/100 \text{ x } 162.5 \text{ lb.}$$

$$= 32.5 \text{ lb.}$$

    - Cement Content = 162.5 – 32.5 = 130 lb.

- FG-SCC (regular SCC with hybrid fibers and 20% GP as cement replacement)
    - All quantities remain same as G-SCC, only addition of fibers is an extra step in this mix.
    - Fiber Content calculation.

1. Steel Fibers = Assumed dosage x volume of the mix

$$= 3.5 \text{ lb./yd}^3 \text{ x } 0.25 = 0.875 \text{ lb.}$$

2. Polypropylene Fibers = Assumed dosage x volume of the mix

$$= 1.5 \text{ lb./yd}^3 \text{ x } 0.25 = 0.375 \text{ lb.}$$

References

Ahmed, S., Bukhari, I. A., Siddiqui, J. I., & Qureshi, S. A. (2006). A STUDY ON PROPERTIES OF POLYPROPYLENE FIBER REINFORCED CONCRETE. *31st Conference on OUR WORLD IN CONCRETE & STRUCTURE*, 10.

ACI Committee 237 (2007), Self-Consolidating Concrete. Technical Documents, 34, www.concrete.org

ASTM A820 / A820M-11, Standard Specification for Steel Fibers for Fiber-Reinforced Concrete, ASTM International, West Conshohocken, PA, 2011, www.astm.org

ASTM C39 / C39M-18, Standard Test Method for Compressive Strength of Cylindrical Concrete Specimens, ASTM International, West Conshohocken, PA, 2018, www.astm.org

ASTM C78 / C78M-18, Standard Test Method for Flexural Strength of Concrete (Using Simple Beam with Third-Point Loading), ASTM International, West Conshohocken, PA, 2018, www.astm.org

ASTM C494 / C494M-19, Standard Specification for Chemical Admixtures for Concrete, ASTM International, West Conshohocken, PA, 2019, www.astm.org

ASTM C496 / C496M-04, Standard Test Method for Splitting Tensile Strength of Cylindrical Concrete Specimens, ASTM International, West Conshohocken, PA, 2004, www.astm.org

ASTM C617 / C617M-15, Standard Practice for Capping Cylindrical Concrete Specimens, ASTM International, West Conshohocken, PA, 2015, www.astm.org

ASTM C1116 / C11116M-06, Standard Specification for Fiber-Reinforced Concrete, ASTM International, West Conshohocken, PA, 2006, www.astm.org

ASTM C1611 / C1611M-05, Standard Test Method for Slump Flow of Self Consolidating Concrete, ASTM International, West Conshohocken, PA, 2005, www.astm.org

ASTM C1866 / C1866M-20, Standard Specification for Ground-Glass Pozzolan for Use in Concrete, ASTM International, West Conshohocken, PA, 2020, www.astm.org

ASTM D7508 / D7508M-20, Standard Specification for Polyolefin Chopped Strands for Use in Concrete, ASTM International, West Conshohocken, PA, 2020, www.astm.org

ASTM E119-19, Standard Test Methods for Fire Tests of Building Construction and Materials, ASTM International, West Conshohocken, PA, 2019, www.astm.org

ASTM F2170-19a, Standard Test Method for Determining Relative Humidity in Concrete Floor Slabs Using in situ Probes, ASTM International, West Conshohocken, PA, 2019, www.astm.org

Charles E. Whitley, P. (2019). *The Effects of Fire on Concrete*. <<https://www.edtengineers.com/blog-post/fire-effects-concrete >> (Last accessed November 1, 2021)

Constructionor. (2015). *Glass Fiber Reinforced Concrete (GFRC)*. <<https://constructionor.com/glass-fiber-reinforced-concrete-gfrc/#:~:text=1%20In%20many%20environmental%20conditions%20when%20exposed%20to,is%20more%20resistant%20to%20freeze-melting%20than%20normal%20concrete. >> (Last accessed Noveember 6, 2021)

Crafting with concrete (2021). *What is glass fiber reinforced concrete?* <<https://craftingwithconcrete.com/what-is-glass-fiber-reinforced-concrete/ >> (Last accessed November 7, 2021)

Ding, Y., Azevedo, C., Aguiar, J. B., & Jalali, S. (2012). Study on residual behaviour and flexural toughness of fibre cocktail reinforced self compacting high performance concrete after exposure to high temperature. *Construction and Building Materials 26*, 11.

Ehrlich, B. (2010). *Reducing Environmental Impacts of Cement and Concrete*. <<https://www.buildinggreen.com/feature/reducing-environmental-impacts-cement-and-concrete >> (Last accessed November 2, 2021)

Euclid Chemicals. (2021). *PLASTOL SPC.* << https://www.euclidchemical.com/fileshare/ProductFiles/TDS/Plastol_SPC.pdf >> (Last accessed November 8, 2021)

Euclid Chemicals. (2021). *PSI FIBERSTRAND 100.* <<https://www.euclidchemical.com/fileshare/ProductFiles/TDS/PSI_Fiberstrand_100.pdf >> (Last accessed November 8, 2021)

Euclid Chemicals. (2021). *PSI STEEL FIBER C6560.* <<https://www.euclidchemical.com/fileshare/ProductFiles/TDS/PSI_Steel_Fiber_C6560.pdf >> (Last accessed November 8, 2021)

Garside, M. (2021). *Major countries in worldwide cement production from 2010 to 2020*. <<https://www.statista.com/statistics/267364/world-cement-production-by-country/ >> (Last accessed November 5, 2021)

Ghafoori, N., Sharbaf, M. R., Najimi, M., & Batilov, I. (2016). Natural Pozzolan Contained Self-Consolidating Concrete. *Fourth International Conference on Sustainable Construction Materials and Technologies*, (p. 12). Las Vegas, USA.

Greenspec. (2021). *The Environmental Impacts of Concrete*. <<https://www.greenspec.co.uk/building-design/environmental-impacts-of-concrete/>> (Last accessed November 9, 2021)

Helal, M. A., & Heiza, K. M. (2010). Effect of Fire and High Temperature on the Properties of Self Compacted Concrete. *CICE 2010 - The 5th International Conference on FRP Composites in Civil Engineering*, 2.

Islam, G. S., Rahman, M. H., & Kazi, N. (2017). Waste glass powder as partial replacement of cement for sustainable concrete practice. *International Journal of Sustainable Built Environment*, 8.

Kaminsky, A., Kristic, M., Rangaraju, P., Tagnit-Hamou, A., & Thomas, M. D. (2020). Ground-Glass Pozzolan for Use in Concrete. 9.

Li, Y., Yang, E.-H., & Tan, K. H. (2020). Flexural behavior of ultra-high performance hybrid fiber reinforced concrete at the ambient and elevated temperature. *Construction and Building Materials 250*, 11.

Mishra, G. (2021). *Fiber Reinforced Concrete - Types, Properties and Advantages of Fiber Reinforced Concrete*. <<https://theconstructor.org/concrete/fiber-reinforced-concrete/150/>> (Last accessed November 8, 2021)

Mahapatra, C. K., & Barai, S. V. (2019). Temperature impact on residual properties of self-compacting based hybrid fiber reinforced concrete with fly ash and colloidal nano silica. *Construction and Building Materials 198*, 13.

Nasry, O., Samaouali, A., Belarouf, S., Moufakkir, A., Idrissi, H. S., Soulami, H., . . . Alaoui, A. H. (2021). Thermophysical Properties of Cement Mortar Containing Waste Glass Powder. *Crystals*, 12.

Ning, X., Ding, Y., Zhang, F., & Zhang, Y. (2015). Experimental Study and Prediction Model for Flexural Behaviour of Reinforced SCC Beam Containing Steel Fibers. *Construction and Building Materials 93*, 25.

Persson, B. (2004). Fire resistance of self-compacting concrete, SCC. *Materials and Structures, Vol. 37*, 11.

Robl, T. L., & McCormick, C. J. (2021). *We Are Running Out of Fly Ash: The Nature of Regional Supply Problems.*

Rodriguez, J. (2021, July 8). *Uses, Benefits, and Drawbacks of Fly Ash in Construction*. Retrieved from the spruce: https://www.thespruce.com/fly-ash-applications-844761

Tapia, E. G. (2020). FLEXURAL LOAD CAPACITY OF HEAT-TREATED CONCRETE MIXED WITH RECYCLED GLASS AGGREGATE AND GLASS POZZOLAN.

Varona, F. B., Baeza, F. J., Bru, D., & Ivorra, S. (2018). Evolution of the bond strength between reinforcing steel and fiber reinforced concrete after high temperature exposure. *Construction and Building Materials 176*, 12.

Vitro Minerals. (2020). *VCAS Type GE White Pozzolans.* <<https://www.vitrominerals.com/wp-content/uploads/2020/06/VCAS-Type-GE-White-Pozzolans-TDS-200601.pdf >> (Last accessed November 9, 2021)

Vitro Minerals. (2020). *VCAS White Pozzolans*. (2020). <<https://vitrominerals.com/products/recycled-glass-powders/vcas-white-pozzolans/ >> (Last accessed November 9, 2021)

Wu, H., Lin, X., & Zhou, A. (2020). A review of mechanical properties of fibre reinforced concrete at elevated temperatures. *Cement and Concrete Research 135*, 21.

Yan, L., Xing, Y. M., & Li, J. (2012). The Influence on High-temperature Mechanical Properties of Hybrid-fiber-reinforced High-performance Concrete and Microscopic Analysis. *Applied Mechanics and Materials Vols. 226-228*, 7.

Zheng, W., Li, H., & Wang, Y. (2012). Compressive stress–strain relationship of steel fiber-reinforced reactive powder concrete after exposure to elevated temperatures. *Construction and Building Materials 35*, 10.

Zidol, A., Tognonvi, M. T., & Tagnit-Hamou, A. (2017). Effect of Glass Powder on Concrete Sustainability. *New Journal of Glass and Ceramics*, 14.